Doctoral Dissertation
Doctoral Program in Chemical Engineering (35th Cycle)

Technical Feasibility Study of the Treatment of Liquid Waste from the Oil & Gas Industry with Membrane-based Techniques

Madina Mohamed Mahmmod

* * * * * *

Supervisors:
Prof. Alberto Tiraferri, Department of Environment, Land, and Infrastructure Engineering (DIATI)
Dr. Marco Tagliabue, Department of Research and Development Innovation, ENI

Politecnico di Torino
25 June 2024

This thesis is licensed under a Creative Commons License, Attribution - Noncommercial - NoDerivative Works 4.0 International: see www.creativecommons.org. The text may be reproduced for non-commercial purposes, provided that credit is given to the original author.

I hereby declare that the contents and organisation of this dissertation constitute my own original work and does not compromise in any way the rights of third parties, including those relating to the security of personal data.

Madina Mohamed

.....

Madina Mohamed Mahmmod

Turin, June 25, 2024

Summary

Environmental challenges related to the management of complex aqueous liquids related to the various phase of hydrocarbon-based energy production are many and diverse. Compared to traditional treatment methods, membrane processes may offer an environmentally friendly alternative under some circumstances, due to their high selectivity, scalability, and cost efficiency. This dissertation investigates the application of membrane technology in the context of oil and gas aqueous by-product treatment and used lubricant oil (ULO) recovery.

The dissertation is divided into 3 chapters. Chapter 1 investigates the potential utilization of a forward osmosis-based system combined with nanofiltration to concentrate produced water and extract freshwater. High recovery experiments are discussed, followed by nanofiltration applied on the diluted draw solution to regenerate it and achieve a final freshwater product. Chapter 2 examines instead forward osmosis for a different application, namely, for amine water volume reduction (dewatering). In this case, the process does not aim at extracting freshwater but to concentrate the amine water as much as possible, without necessarily recover the draw agent. Chapter 3 studies the purification of used lubricant oil (ULO) obtained from oil & gas industry with porous ultrafiltration ceramic membranes. Using real ULO samples, different native and grafted membranes are investigated to understand the effect of pore size, membrane surface modification, and different test conditions (e.g., pressure, temperature, and crossflow).

Improper liquid waste treatment and disposal from oil & gas industry can have both environmental and economic detrimental effects. This study focused on the use of membrane technology for the treatment of produced water, amine water,

and used lubricant oils. Synthetic produced water and amine water were experimented using forward osmosis. Ultrafiltration was the method of choice for experimenting on the treatment and recovery of used lubricant oils. Overall, these methods provided viable treatment solutions to waste liquids from the oil & gas industry, with each method having its own merits. It is crucial, however, to also highlight the challenges for each method used, and the viable solutions and/or further studies that can overcome those challenges.

The process of forward osmosis followed by nanofiltration for the treatment of synthetic produced water and the regeneration of the draw solution is only partly technically viable. $MgCl_2$ was tested as draw agent at various osmotic pressures and draw-to-feed ratios in order to determine the ideal parameters to achieve the highest recovery, with modelling to validate the data and to explore different conditions. The combination of FO followed by NF achieved up to 73% water recovery for the specific feed solution investigated, but with important loss of draw agent, which suggests the need to replenish the draw agent continuously. Also, the results suggest the potential need of using reverse osmosis membranes instead of NF membranes for the draw agent recovery. Further improvements to this study may include the use of real produced water samples and economic calculations to gain insight into the economic viability of the most promising configurations.

Concentration of amine water (a byproduct of gas sweetening processes) was experimented using forward osmosis. The most suitable draw solution (NaCl) was used for high recovery experiments. Varying osmotic pressure and draw-to-feed volume ratios, experimental and simulated results were combined to estimate achievable recovery rate under a broad range of operating conditions, once again supported by modelling by deploying the analytical FO equations. High osmotic

pressure combined with larger initial DS-to-FS volume ratio yielded higher recovery rates, with the highest recovery achieved being 55%. Counter-current configuration proved as superior to co-current configuration in terms of system efficiency. Nevertheless, it is important to note that higher osmotic pressures would ultimately result in increased operational costs and possible complications in managing or discharging the effluent draw solution. The membrane mostly succeeded in preventing reverse flux, with high retention rate of total organic carbon (TOC) and total nitrogen (TN) observed. Overall, FO demonstrated medium to high potential in dewatering amine water; however, challenges, such as membrane fouling (which requires constant cleaning and/or membrane changeout depending on operating conditions) still stand. Overall, the practical application of this method would require careful study of the system objectives, costs, and legal limitations.

Finally, several lab scale tests were performed for the recovery of ULO using UF membranes with different pore sizes (10 nm, 30 nm, and 5 nm). The obtained results showed that suitable purity, yield, and viscosity retention were achieved using the 10 nm ceramic UF membranes. This was further examined using not only native ceramic membranes, but also grafted ceramic membranes. In addition, different feed oils were tested; clean lube oil, base oil, ULO after a first pre-treatment (using a distillation column), ULO after a second pre-treatment (using a second distillation column), and crude ULO. Tests performed using clean lube oil as a feed showed a stable flux with time, with no observable influence of membrane pore size or grafting chemistry. In addition, up to 100% removal of several metals, such as Ca, Mg, and Mo was observed, while other elements, such as P, Zn, and Fe, were partially removed. High declining fluxes were obtained when

testing base oil as the feed stream with native membranes. Moreover, fluxes were pore size dependent. Finally, testing different ULO with different pre-treatment as feed streams using native 10 nm membrane resulted in a stable flux that was independent from the feed type. High removal of metals, such as Ca, Mg, and Mo was observed, while other elements, such as P, S, Zn, Si, were retained at a lower rate by the membrane, similar to the results obtained for the clean lube oil.

Based on the conducted literature review and experimental results of this study, membrane technology demonstrates technical promise in treatment of different liquid streams and from the oil & gas industry. While the experimental results highlight the positive outcomes, it is vital to consider economic and legal limitations in managing the effluent solutions that may require further treatment before safely discharging into the environment.

Acknowledgement

This research was funded by Politecnico di Torino and by Eni S.p.a. through a Ph.D. scholarship to Madina Mohamed.

I would like to express my deepest gratitude to all those who supported me throughout my dissertation journey. Without their encouragement and love, this work would not have been possible. First and foremost, I would like to thank my mother for her unwavering support, love, and wisdom. she has been my constant source of strength, always offering encouragement and believing in my potentials, even in the most challenging times. To my siblings, Eslam and Ayaat, thank you for always being by my side during both challenging and joyful times. I am eternally grateful to my husband, whose patience, understanding, and encouragement was invaluable. Your support has been nothing short of extraordinary.

To my friends, Mennat, Yasmine, Dina, Mariam, Sophia, Norca, and Djalila, thank you for your emotional support, words of encouragement, and for always reminding me of the bigger picture during the most stressful times. Your friendship has meant the world to me.

To my precious daughter, your joy, laughter, and love were the light that brightened even the toughest days. you inspire me to strive for greatness and remind me of what truly matters in life. I dedicate this work to you.

Finally, I would like to express my deepest gratitude to my supervisor, Prof. Alberto Tiraferri, for his exceptional guidance and unwavering support throughout the course of my dissertation. I truly appreciate your patience, encouragement, and commitment to my academic growth. Thank you for being such an inspiring mentor. To Dr. Marco Tagliabue, thank you for your insightful advice and constructive suggestions. I appreciate the time and effort you invested in guiding me through this process.

Thank you all for being part of this journey.

Table of Contents

Summary 0

Acknowledgement 1

Table of Contents 1

List of Figures 3

List of Tables 4

Introduction 1

Chapter 1: Technical Feasibility of Extraction of Freshwater from Produced Water with Combined Forward Osmosis and Nanofiltration 4

1. Introduction 4

2. Materials and Methods 8

2.1. Membranes and Chemicals 8

2.2. Feed Solution Characteristics 9

2.3. Lab-Scale Membrane Filtration Setups 9

2.4. FO and NF Tests 11

2.5. Water Characterization 15

2.6. FO and NF Water Flux Simulations 15

3. Results and Discussion 17

3.1. Choice of the Draw Solute and Operating Conditions 17

3.2. Observed Productivity of the FO Step and Validation of the Water Flux Simulations 18

3.3. Predicted Productivity of the FO Step 22

3.4. Draw Solution Regeneration and Freshwater Extraction with Nanofiltration 26

3.5. Quality of the Product Water 28

4. Conclusion 30

Chapter 2: Technical Feasibility of the Concentration of Amine Water using Forward Osmosis 33

1. Introduction 33

2. Literature and Patent Review 35

3. Materials and methods 42

3.1. Membranes and Chemicals 42

3.2 Feed solution characteristics 43

3.3 Lab-scale membrane filtration setup 43
3.4 FO tests 43
4. Results and Discussion 45
4.1 Choice of the draw solute and operating conditions 45
4.2 Observed productivity of the FO step and validation of the water flux simulations 47
4.3 Predicted productivity of the FO step 49
4.4 Quality of the product water 52
5. Conclusion 53
Chapter 3: Preliminary Technical Feasibility Study of the Recovery of Used Lubricant Oil (ULO) from Oil & Gas Industry Using Ultrafiltration 56
1. Introduction 56
2. Materials and methods 60
2.1 Membranes and chemicals 60
2.2 Feed Solutions Characteristics. 62
2.3 Properties of different ULOs in this study 64
2.4 Membrane filtration setup 65
2.5 UF tests and varying operational parameters tests. 66
3. Results of Clean Lubricant Oil 67
3.1 Effect of membrane grafting and pore size 67
3.2 Filtration performances of the native 10 nm membrane for clean lubricant oil 70
3.3 Effect of Temperature for Native 10 nm 71
3.4 Effect of Pressure for Native 10 nm 72
4. Results of base oil OSIL150 74
Filtration performances of the 5, 10, and 30 nm membrane for OSIL150 74
5. Results of ULO feed streams 75
Filtration performances of the 10 nm membrane for different ULO feed streams 75
6. Effect of Crossflow Velocity 77
7. Conclusion 78
Conclusions 80
References 83

List of Figures

Figure 1: schematic diagram of the lab-scale forward osmosis (FO) system (Created with BioRender.com) 10
Figure 2: Simulated recovery rates vs. experimentally observed recovery rates for each tested condition of DS initial osmotic pressure and DS-to-FS-initial-volume ratio. 18
Figure 3: Water fluxes measured (data points) and simulated (lines) in forward osmosis as a function of water recovery rate. 19
Figure 4: Productivity of an FO system simulated under co-current vs. counter-current configurations. 23
Figure 5: Simulation-based predictions of FO system behavior and productivity in co-current configuration, as a function of DS influent osmotic pressure and DS-to-FS-influent-flow-rate ratio. 25
Figure 6: Water fluxes in nanofiltration as a function of relative recovery rate 27
Figure 7: (a) obtained water flux as a function of DS concentration / (b) NaCl and MgCl2 analytical FO water flux model when used as DS. 46
Figure 8: Water fluxes measured (data points) and simulated (lines) in forward osmosis as a function of water recovery rate. 47
Figure 9: Productivity of an FO system simulated under co-current vs. counter-current configurations. 50
Figure 10: Simulation-based predictions of FO system behavior as s function of DS influent osmotic pressure and DS to FS influent flow rate ratio 52
Figure 11: Illustration of ceramic membranes Grignard modification 62
Figure 12: Different feeds used in the UF. All membranes were tested using the clean commercial lubricant oil, while industrial ULO process streams from Osilub were only tested with a selected set of membranes. 64
Figure 13: Crossflow lab scale setup system 65
Figure 14: Clean lubricant oil before and after UF treatment using 10 nm native membrane..... 71
Figure 15: Effect of temperature on flux & reverse dynamic viscosity of clean lubricant oil during UF. 72
Figure 16: Effect of pressure on flux of clean lubricant oil during UF. 73
Figure 17: Effect of crossflow velocity on flux of OSILUB2 during UF..... 77

List of Tables

Table 1: Characteristics of the synthetic produced water used as feed solution 9
Table 2: Summary of water flux and recovery results in the FO and NF tests. 21
Table 3: Composition of the final product water from combined FO and NF filtration tests. 30
Table 4: Characteristics of the synthetic amine water used as feed solution.. 43
Table 5: Summary of water flux and recovery results in the FO..... 48
Table 6: Composition of the diluted draw solutions from the high-recovery FO tests 53
Table 7: Typical composition of ULO..... 56
Table 8: Ceramic UF membranes with different grafting for used lubricant oil purification. 62
Table 9: Characteristics of the ULOs 64
Table 10: Metal content of different ULOs (Additives, wear, and contaminations content)..... 65
Table 11: Membranes' performances using clean lubricant oil as feed 69
Table 12: Characteristics of the feed, retentate, and permeate of clean lubricant oil after UF..... 70
Table 13: metal content of the treated clean lubricant oil using 10 nm membrane (Additives, wear, and contaminations content) 70
Table 14: 10 nm membrane performance at various temperature and constant pressure (10 bar) 72
Table 15: 10 nm membrane performance at various pressure and constant temperature (110°C) 73
Table 16: Fluxes and water retention of the 5, 10, and 30 nm membrane for OSIL150..... 74
Table 17: Characteristics of the feed, retentate, and permeate of OSIL150 using 10 nm UF membrane. 75
Table 18: Characteristics of ULO feed streams after UF using 10 nm membrane. 76
Table 19: Metal content of the treated ULO feed streams using 10 nm membrane (Additives, wear, and contaminations content)..... 76
Table 20: Metal rejection of the treated ULO feed streams using 10 nm membrane..... 77

Introduction

The oil and gas industry still plays an important role in meeting the high energy demands required to sustain contemporary lifestyle. For the production of hydrocarbon-based energy sources, such as oil, gas, coal bed methane, and shale oil and gas, deep drilling of earth's crust is required for their extraction. During the extraction process, significant volumes of water are produced as a by-product, which is typically referred to as produced water (PW). The age of the reservoir, the location of the well, and the type of extraction determine the amount and composition of PW. The older the reservoir, the larger the volume of PW, which might constitute up to 98% of the total fluid volume extracted from the ground. In the majority of the oil wells, a water-to-oil ratio of 1:3 is usually observed. The constituents of PW are also influenced by the surrounding natural geological formations, but commonly comprise suspended solids, organic matter, and different soluble mineral ions. Other factors affecting the specific composition of PW are chemical additives used in the oil gas operations according to production methods. [1,2]

Extraction is just the first phase of hydrocarbon-based energy production. Before crude oil and natural gas can be used, they must undergo specific processing. In the case of natural gas, it is either partially or completely processed to remove impurities, including hydrogen sulfide (H_2S) and carbon dioxide (CO_2), which pose significant safety risks [3]. H_2S is particularly hazardous even at low concentrations and must be removed before natural gas can be transported or commercially distributed. Among the methods used for H_2S and CO_2 removal from natural gas (a process known as sweetening) is the use of aminated compounds. Amines and alkanolamines, such as

N-methyldiethanolamine (MDEA), are commonly employed to wash raw natural gas, forming salts that are later thermally decomposed [3,4]. This process allows for the recycling of washing solutions and the release of gaseous hydrogen sulfide, often directed to a Claus reactor. However, the aqueous solutions of tertiary alkanolamines degrade over time due to repeated washing and regeneration cycles, necessitating periodic replacement [5,6]. The resulting liquid, referred to as "amine water," has a high pH (often greater than 12.0) and contains significant amounts of organic and inorganic compounds, corrosion by-products, and other impurities. Handling and treating amine water present numerous challenges for natural gas plants, including corrosion of metal pipelines and components, accumulation of organic acids from foaming, as well as solvent loss at high temperatures due to amine vapor pressure. Typically, amine water is either sent for pyrolysis or for other cumbersome disposal, which can be costly, especially if transport by tankers is required [7-9].

Additionally, the disposal of used lubricant oil (ULO), a crucial component in machinery operation within the oil & gas sector, adds another layer of complexity to the environmental impact of hydrocarbon-based energy production. The composition of virgin lubricant oil is often 80-90% base oil, along with chemical additives, such as detergents, viscosity enhancers, antioxidants, and rust and wear inhibitors. Temperature builds up during the use of lubricant oil, which changes the chemistry of the oil and its additives. This phenomenon causes corrosion and oxidation due to additives break down. Concurrently, the change in viscosity, acidity, flash point, and metal content of the oil have a direct effect on the level of impurities in the lubricant oil. Therefore, ULO management and treatment in the oil and gas industry also stand at the forefront of environmental and sustainability concerns [10]. Nevertheless, with

proper recycling and treatment, ULO can be considered a valuable resource, instead of posing only as a potential source of environmental pollution. [10]

As briefly outlined above, environmental challenges related to the management of complex aqueous liquids related to the various phase of hydrocarbon-based energy production are many and diverse. While there is no individual treatment process that can address all these challenges, membrane separation emerges as one of the most promising techniques for addressing the complex composition of liquids generated by the oil and gas sector, as well as the challenges posed by ULO. Compared to traditional treatment methods, membrane processes may offer an environmentally friendly alternative under some circumstances, due to their high selectivity, scalability, and cost efficiency. This dissertation investigates the application of membrane technology in the context of oil and gas aqueous by-product treatment and ULO recovery.

Chapter 1 investigates the potential utilization of a forward osmosis-based system combined with nanofiltration to concentrate produced water and extract freshwater. High recovery experiments are discussed, followed by nanofiltration applied on the diluted draw solution to regenerate it and achieve a final freshwater product. Chapter 2 examines instead forward osmosis for a different application, namely, for amine water volume reduction (dewatering). In this case, the process does not aim at extracting freshwater but to concentrate the amine water as much as possible, without necessarily recover the draw agent. Chapter 3 studies the purification of used lubricant oil (ULO) obtained from oil & gas industry with porous ultrafiltration ceramic membranes. Using real ULO samples, different native and grafted membranes are investigated to understand the effect of pore size, membrane surface modification, and different test conditions (e.g., pressure, temperature, and crossflow).

Chapter 1: Technical Feasibility of Extraction of Freshwater from Produced Water with Combined Forward Osmosis and Nanofiltration[1]

1. Introduction

Petroleum and other underground energy resources still play a substantial role in the modern economy [11]. While society is transitioning toward the use of alternative resources [12], almost all industries currently depend on petroleum products at one stage or another, e.g., fuel production or petrochemical manufacturing. Other than the final high-value products, oil and gas extraction and processing produce a considerable number of low-value ones. A chief example is produced water (PW) [13–17]. Produced water is a complex brine brought to the surface along with hydrocarbons, which later combines with minor condensates and mixed water streams that originated in the separation processes of hydrocarbons. Globally, 248.4 million barrels of PW are generated from oil production per day, from both onshore and offshore wells [17–20].

Two common handling methods of PW are disposal and reuse [16,21,22]. The latter exploits PW as a potential freshwater resource [16], according to United Nations Sustainable Development Goals 6 and 12* [https://sdgs.un.org/goals (accessed on 29 April 2024)]. However, a suitable treatment of PW is required, depending on the specific application, e.g., process, potable, sanitary, and crops irrigation. The applications can range from reinjection into oil or gas reservoirs for enhanced oil

[1] The contents of this chapter were published on May 2024 in "Membranes 2024" journal under the following citation: Mohamed, M.; Tagliabue, M.; Tiraferri, A. Technical Feasibility of Extraction of Freshwater from Produced Water with Combined Forward Osmosis and Nanofiltration. Membranes 2024, 14, 107. https://doi.org/10.3390/membranes14050107

* https://sdgs.un.org/goals (accessed on 29 April 2024)

recovery to, potentially, high-end uses in the agricultural and civil sectors [23]. PW requires intensive treatment to be used outside the energy sector, such as for irrigation purposes, even when these do not involve crops or products for human consumption [22]. Therefore, it is essential that a series of strategies are developed for PW treatment and for the extraction of water to comply with the necessary standards [15,24,25].

Various methods are being employed or developed aimed at the treatment of PW [19,26]. Among those or in the framework of certain management schemes, membrane separation processes may provide scalability and a suitable separation performance [18,21,25,27–43]. The complexity of the PW composition presents a challenging task in selecting suitable unit operations for its treatment. Microfiltration or ultrafiltration using ceramic or polymeric membranes, though effective in removing suspended materials, demand post-treatment to enhance the quality of the treated effluent, e.g., denser membrane separation steps [20,30,35,40,44]. Reverse osmosis is impractical for many PWs due to their high salinity and composition, since typical PWs contain non-soluble oil/organics and chemicals that would render intensive pre-treatment necessary prior to the RO step. These characteristics would limit the productivity, the recovery rate, and/or the permeate quality in RO [41,45,46]. Membrane distillation offers opportunities for treating highly saline solutions, but with high energy expenses [36,47]. Numerous researchers have employed a hybrid approach that integrates membrane filtration with other processes to improve the effluent quality and system efficiency. As representative examples, Purnima et al. reported that microfiltration followed by biological treatment removed 99% of organic matter rather than using a single operation unit [20]. Riley et al. introduced a hybrid membrane biosystem that was able to remove over 99% of organic matter and 94% of TDS from PW [25].

Forward osmosis is an osmotically driven membrane technology that has been suggested as a valid tool for the treatment of PW under certain circumstances, especially combined with other treatment units [29,31,32,37,38,48–60]. The driving force of the water transport in an FO process is owed to the inherent osmotic pressure difference across the membrane. A draw solution (DS) facilitates the freshwater passage from the feed solution (FS), which has a comparatively lower salinity and ultimately lower osmotic pressure than the DS. Indeed, in order to maintain the driving force and ensure the continuous, feasible, operation of the FO system, the diluted draw solution must be reconcentrated after its dilution, a step that simultaneously allows water extraction [61]. Such a second system step depends on the nature and the concentration of the draw agent to be reconcentrated and represents the energy-intensive unit operation within the water recovery scheme. An interesting aspect of this approach is that it provides a dual barrier for contaminant removal, whereby one step, namely, the FO unit treatment, requires little energy [62]. Moreover, while not widely implemented, FO is presently a mature technology, with reliable providers able to provide installation on a medium and large scale [63].

A number of past studies have investigated the implementation of FO in the treatment of PW, but the technical feasibility of this strategy has not been fully understood [64]. Nawaza et al. investigated the efficiency of a combined FO–membrane-distillation system for the treatment of four different PW streams sourced from a single industrial site [53]. The water–oil stream served as the DS for FO with measured water fluxes ranging from 8.3 L $m^{-2}h^{-1}$ (LMH) to 26.8 LMH in the FO step, and 5.6 LMH to 11.1 LMH in the membrane distillation step. Stable fluxes in both FO and membrane distillation were achieved, with minimal fouling and adequate product

water quality. One prominent issue that hinders the investigated system is that membrane distillation is not yet a mature technique. In another study conducted by Chen et al., the effectiveness of two FO membranes, a commercial cellulose triacetate membrane and a custom-made thin film composite (TFC) membrane, was evaluated for treating shale gas drilling flow-back fluids [65]. Using a synthetic brine as the DS, the TFC membrane provided higher fluxes but was also affected by fouling problems, compared to the cellulose triacetate membrane. Another relevant study conducted by Minier-Matar et al. assessed the use of FO for the concentration of PW aimed at its disposal by deep well injection. Two main operating parameters were investigated in this study, namely, the DS concentration (from 35 to 175 g/L NaCl) and temperature. The experimental findings showed that a 50% volume reduction in PW was achieved with a stable flux of 12 LMH using 1 M NaCl as the draw solution. Organic matter from the FS did not transfer considerably into the diluted DS, thus minimizing its discharge into the environment. However, neither study evaluated DS reconcentration [52].

The aim of the current study is to provide further insight into the technical feasibility of a system comprising FO and nanofiltration (NF) for the extraction of freshwater from PW and for the regeneration of the DS. The discussion starts with data obtained in laboratory-scale experiments and centered around the water fluxes and water quality observed under high-recovery experiments. For simplicity, a synthetic PW is used. The experimental data are then deployed to validate the analytical, system-scale modeling of both units, namely, FO and NF, thus allowing an investigation of conditions that would also fall outside those investigated experimentally. The scope of this work is partly limited by the use of a synthetic FS and by the scale of the

experiments, but the results and analyses provide a benchmark for the assessment of the technical feasibility, or lack thereof, of an FO-based system in the management of typical PW of streams with similar salinity and composition.

2. Materials and Methods

2.1. Membranes and Chemicals

Thin-film composite polyamide membranes were purchased for the FO experiments. Following the protocol reported previously by Tiraferri et al. [66], membrane characterization was performed to determine the active layer water permeance, A, NaCl permeability coefficient, B, and the support layer structural parameter, S, using $MgCl_2$ as a draw solute and deionized water as the feed solution. membrane characterization was performed on a number of separate samples (>4) using a laboratory-scale FO system to determine the active layer water permeance, *A*, the $MgCl_2$ permeability coefficient, *B*, and the support layer structural parameter, *S*. $MgCl_2$ was used as the draw solute of choice for such characterization and deionized water as the feed solution. The values obtained were 2.74 ± 0.50 LMH, 0.07 ± 0.25 LMH, and 427 ± 19 μm, respectively. The membrane performance was robust, and the values obtained with different samples fit within an adequate range. For the NF tests, flat-sheet DuPont NF90 membranes were purchased from Oltremare (Fano, Italy).

The solutions were prepared using magnesium chloride hexahydrate ($MgCl_2 \cdot 6H_2O$, purity ≥ 99.8%), calcium chloride (purity ≥ 99.8%), sodium acetate, boric acid, and sodium chloride (NaCl) (purity ≥ 99.8%), purchased from Carlo Erba (Italy), sodium sulfate (purity ≥ 99%) purchased from Chem-lab, and potassium chloride (KCl) (purity ≥ 99%) purchased from Sigma Aldrich. Acetic acid (purity ≥

99.8) was used for adjusting the feed solution pH and was purchased from Carlo Erba. Three different draw agents were preliminarily assessed, namely, sodium chloride, magnesium chloride, and sodium propanoate (purity ≥ 99.8%) purchased from Carlo Erba. DI water from a Milli-Q (Merck, Italy) system was used in all preparations.

2.2. Feed Solution Characteristics

The feed solution used in this study was synthesized to simulate the composition of pre-treated PW, e.g., de-oiled, filtrated, and degassed. Table 1 presents the main characteristics of the feed solution.

Table 1: Characteristics of the synthetic produced water used as feed solution

Parameter	Produced water
pH	7.8
Conductivity (µS/cm)	61741
Na^+ (ppm)	2700
Ca^{2+} (ppm)	1500
K^+ (ppm)	500
Mg^{2+} (ppm)	500
Acetic acid (ppm)	4700
Cl^- (ppm)	8500
SO_4^{2-} (ppm)	1300
$B(OH)_3$ (ppm)	60

2.3. Lab-Scale Membrane Filtration Setups

The FO lab-scale plant was purchased from Sterlitech Corporation (Kent, WA, USA). As shown in Figure 1, It is composed of two reservoirs for the FS and the DS, respectively, with a capacity of 7 L each. It includes a membrane cell (acrylic Sepa cross-flow cell, Sterlitech, Auburn, WA, USA) with dimensions 146 mm long, 94.5

mm wide, and 1.5 mm deep. The active area of the membrane sample was 140 cm^2. The membrane was used in the so-called "FO mode", with the active layer facing the FS and the support layer facing the DS. The system comprises two variable speed gear pumps (Cole-Parmer, Vernon Hills, IL, USA), one for each stream loop, and a data acquisition system. The DS tank was placed on a digital scale balance (Kern Instruments, Balingen, Germany) connected to a computer to record the change of volume during the experiment, and, hence, calculate the water flux. For all the experiments, the crossflow rate was 1.8 L/min for both the feed and the draw sides, while the temperature of both streams was maintained at 21 ± 1 °C by submerging in the two tanks stainless-steel heat exchanger coils connected to an external chiller. Both the FS and the DS streams were recirculated back to the respective reservoirs during the experiments.

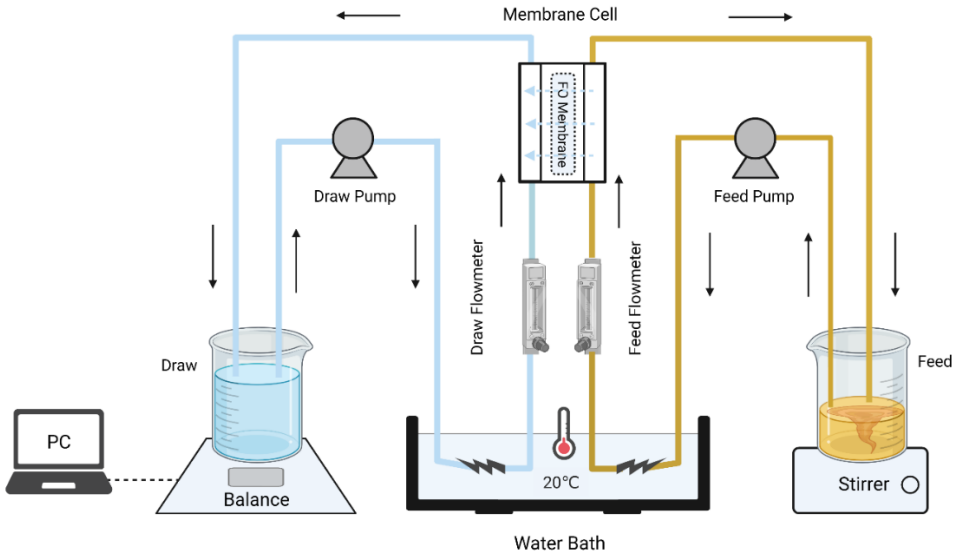

Figure 1: schematic diagram of the lab-scale forward osmosis (FO) system (Created with BioRender.com)

A crossflow NF system was used for conducting all draw agent regeneration experiments. The unit is composed of a high-pressure pump (Hydra-cell pump, Wanner

Engineering, Inc., Minneapolis, MN, USA), feeding reservoir, flat-sheet membrane housing cell (stainless steel Sepa cross-flow cell, Sterlitech, Auburn, WA, USA), temperature control, and data acquisition system. The housing cell comprises a channel with length 147 mm, width 97 mm, and height 1.9 mm. The membrane active area was thus 140 cm^2. A floating disc rotameter was utilized to monitor the crossflow rate. Both the crossflow and operating pressure were controlled and adjusted by means of a bypass valve and a back-pressure regulator (Swagelok, Solon, OH, USA), while a computer-interfaced balance automatically monitored and recorded the permeate flow rate every 1 min. The retentate streams were recirculated back to the respective reservoir, while the permeate stream was collected in an external tank placed on a computer-interfaced balance. The temperature in the retentate tank was controlled via a recirculating chiller (Model MC 1200, Lauda, Lauda-Königshofen, Germany) accompanied with a stainless-steel coil heat exchanger submerged in the tank to maintain the temperature at 21 ± 1 °C.

2.4. FO and NF Tests

In preliminary tests, various draw agents were assessed based on their water flux performance in low-recovery tests. Specifically, the synthetic PW (Table 1) was used as FS while measurements of steady-state water fluxes were conducted over five steps, characterized by different values of the DS osmotic pressure. Following the selection of the most suitable draw agent, namely, $MgCl_2$, high-recovery FO tests were performed. A minimum of two replicates were conducted for each test to guarantee experimental repeatability.

The main experimental design of this study consisted of a high-recovery FO test conducted on the synthetic produced water, followed by a high-recovery NF test conducted with the diluted draw solution from the previous FO step. The high-recovery FO tests were conducted as follows: 2.5 L of synthetic PW was used as FS. The initial $MgCl_2$ DS osmotic pressure and/or volume were varied for each experiment. The tested osmotic pressure values were 30, 40, 60, 80, and 120 bar, while the volumes were 2.5 L, 4 L, and 5.5 L, resulting in DS to FS initial volume ratios of 1, 1.6, or 2.2; see Table 2 for a summary of the experimental conditions. Different DS-to-FS-initial-volume ratios in lab-scale tests represent different DS-to-FS-influent-flow-rate ratios in real-scale scenarios. The relationship between osmotic pressure and draw agent concentration was obtained using "OLI Studio" software (OLI Systems Inc., Parsippany, NJ, USA). The FS and DS were recirculated back to their respective reservoirs, during which the former was concentrated, and the latter was diluted. The water flux was measured every 10 min until approximately 65–70% of the initial FS volume permeated from the feed to the draw side, or until the flux went to near zero, whichever condition was reached first. Generally, the driving force for the FO phenomenon is the difference in osmotic pressures of the feed and draw solutions across the membrane. During the FO process, water molecules permeate from the feed side to the draw side while solute molecules are rejected by the membrane and consequently, the feed solution is concentrated, and the draw solution is diluted. Due to concentration polarization (CP), the osmotic pressure of the feed is increased at the same time the osmotic pressure of the draw is decreased at the active layer of the membrane. In other words, the bulk osmotic pressure difference will be significantly higher than the effective osmotic pressure difference as a result of CP effect. External

concentration polarization (ECP) and internal concentration polarization (ICP) are two types of CP that induce the reduction of the effective osmotic pressure difference in FO desalination process. As a result of water transport from the feed to the draw, concentrative ECP happens due to the buildup of solutes on the active layer of the membrane which increases the concentration of the feed at the membrane active layer. Eventually, the water flux declines gradually due to the gradual decrease in the net osmotic driving force. Another major factor for flux decline is attributed to dilutive ICP. Dilutive ICP occurs as the draw solute within the porous support layer is diluted by the constant transport of water from the feed to the draw.

The recovery rate from the FO tests, *REC*, was calculated as follows:

$$REC = 1 - \frac{V_{P,tot}}{V_{F,0}}$$

where *V* is the volume of a certain solution, the subscript "*P,tot*" refers to the total permeated volume throughout the test that diluted the draw solution, the subscript "*F,0*" to the initial feed volume at the beginning of the test. The concentration factor, *CF*, relates to the recovery rate as:

$$CF = \frac{1}{1 - REC}$$

The so-called "system rejection" of a species is instead calculated as:

$$R = 1 - \frac{c_{D,fin}}{c_{F,0}}$$

and it takes thus into account the concentration of species in the final draw solution volume with respect to the initial concentration in the feed solution at the beginning of the test.

Following each FO test, the diluted DS was used as solution to be reconcentrated in the NF tests. In the high-recovery NF tests, a 100% relative water recovery rate was targeted; i.e., the same volume of water that had previously diluted the DS was made to permeate the NF membrane. At the beginning of each FO test, an aliquot of the initial FS and DS solutions was sampled. At the end of each FO test, samples were collected from the concentrated FS and the diluted DS, while, at the end of each NF test, the regenerated DS and the permeated products were sampled.

For completeness, the recovery rate from the FO tests, REC^{FO}, and the relative recovery rate from the NF tests, REC_{rel}^{NF}, were calculated, respectively, as follows:

$$REC^{FO} = 1 - \frac{V_{P,tot}^{FO}}{V_{F,0}}$$

$$REC_{rel}^{NF} = 1 - \frac{V_{P,tot}^{NF}}{V_{P,tot}^{FO}}$$

where *V* is the volume of a certain solution, the superscripts "*FO*" and "*NF*" refer to the process producing a certain volume of permeate, the subscript "*P,tot*" refers to the total permeated volume throughout the test, the subscript "*F,0*" to the initial feed volume at the beginning of the test.

The so-called "system rejection" of the draw agent is instead calculated as:

$$R = 1 - \frac{c_{P,tot}^{NF}}{c_{D,0}^{FO}}$$

and it takes thus into account the concentration of a species in the total permeated volume from the NF step and the initial concentration in the draw solution of the FO step at the beginning of the FO tests itself, $c_{D,0}^{FO}$.

2.5. Water Characterization

Elemental analysis on the liquid samples diluted with aqueous nitric acid (HNO_3, Merck, superpure grade) was conducted by inductively coupled plasma optical emission spectrometry (ICP-OES) using a Thermo Fisher ICAP 6000 instrument. The calibration was performed from standards certified by the external calibration method (VWR). Total carbon (TC) was also quantified and used to quantity organic carbon (TOC) with a Shimadzu TOC V CPH analyzer equipped with a Shimadzu NDIR detector. Dissolved anions were quantified by ion chromatography with a Thermo Scientific Dionex ICS 6000 ion chromatograph equipped with an eluent generator (potassium hydroxide, KOH) Thermo Scientific Dionex EGC III, a precolumn Thermo Scientific Dionex Ionpac AG11-HC, a Thermo Scientific Dionex Ionpac AS11 column, and a conductivity meter.

2.6. FO and NF Water Flux Simulations

Simulations of the approximate FO water flux as a function of recovery rate or membrane area were performed by application of the FO water flux equation [61,67]:

$$J_w^{FO} = A\left\{\frac{\pi_D \cdot \exp\left(-\frac{J_w S}{D}\right) - \pi_F \cdot \exp\left(-\frac{J_w}{k^{FO}}\right)}{1 - \frac{B}{J_w}\left[\exp\left(\frac{J_w}{k^{FO}}\right) - \exp\left(-\frac{J_w S}{D}\right)\right]}\right\}$$

where D is the diffusion coefficient of the draw solute in water, π_D and π_F represent the draw and feed bulk osmotic pressures, and k^{FO} is the mass transfer coefficient at the active layer–solution interface, which is a function of the hydrodynamics of the feed channel and was fixed at the value of 40 LMH, which represents the average value computed for the FO cell utilized in this work. The same value for k^{FO} was applied to simulate the experimental results in co-current mode and

to compute the FO productivity in predictive simulations under both co-current and counter-current configurations.

Simulations of the experimental NF water flux as a function of recovery rate were performed by application of the NF water flux equation:

$$J_w^{NF} = A\left[\Delta P - \sigma \cdot \Delta\pi \cdot \exp\left(\frac{J_w}{k^{NF}}\right)\right]$$

where σ is the reflection coefficient, assumed to be equal to 1 for simplicity, ΔP is the applied transmembrane pressure, and k^{NF} is the mass transfer coefficient at the active layer–solution interface, which is a function of the hydrodynamics of the feed channel and was fixed at the value of 100 LMH, which represents the average value computed for the NF cell utilized in this work.

In cross-flow systems, whether FO or NF, the water flux would vary along the membrane module due to the change in driving force. Therefore, the water flux was calculated through the discretization of the theoretical length of the membrane module by numerical iteration of the equations above, to obtain the amount of water passing across the membrane in each discrete portion of the system. For each portion, the concentrations and the resulting osmotic pressure were thus recalculated through mass and flow balances, to obtain the full profiles along the system.

3. Results and Discussion

3.1. Choice of the Draw Solute and Operating Conditions

A series of preliminary FO experiments were conducted with the synthetic PW as FS for the selection of the draw agent and of the operating conditions for the high-recovery experiments. Three draw solutions were assessed, namely, $MgCl_2$, NaCl, and $C_3H_5NaO_2$. The results of the steady-state water flux as a function of the DS concentration are presented in Figure 2. The results of the simulations run by applying the analytical FO water flux model are also displayed for NaCl and $MgCl_2$ as the DS, and plotted as continuous lines in Figure 2. These calculations were performed without any additional fitting parameters other than the previously determined membrane transport parameters, i.e., *A*, *B*, *S*, and the known cross-flow channel mass transfer coefficient, *k*, which was equal to 40 LMH for the FO cell and the cross-flow conditions deployed in the tests. The highest fluxes were observed with NaCl, likely due to its high diffusion coefficient, which reduced the dilutive internal concentration polarization compared to other compounds. Overall, fluxes between 6 and 9 LMH were observed at a DS bulk osmotic pressure of 42 bar, and fluxes between 12 and 18 LMH at a DS bulk osmotic pressure of roughly 95 bar. Note that these preliminary tests also provided experimental validation of the FS bulk osmotic pressure, equivalent to the value of the DS bulk osmotic pressure at which the modeled fluxes went to zero. This value was equal to 16.3 bar. Despite $MgCl_2$ providing lower fluxes than the other two draw agents, flux values were sufficiently close to those obtained with the other agents to make other considerations important. Specifically, $MgCl_2$ is a universally available and relatively inexpensive salt, which may be recovered using tight nanofiltration membranes, whereas other compounds would necessarily require either highly dense

membranes or other less established techniques, e.g., evaporative ones, for recovery. The hypothesis of this work, which also underlies several other research investigations of forward osmosis systems is the following: while nanofiltration on a divalent salt does not necessarily entail a lower energy need than reverse osmosis for the purpose of DS reconcentration, a combination of higher fluxes and rejections may be advantageous in terms of the system compactness and efficacy of draw agent recovery. The following chapters set forth to discuss the results based on this initial hypothesis.

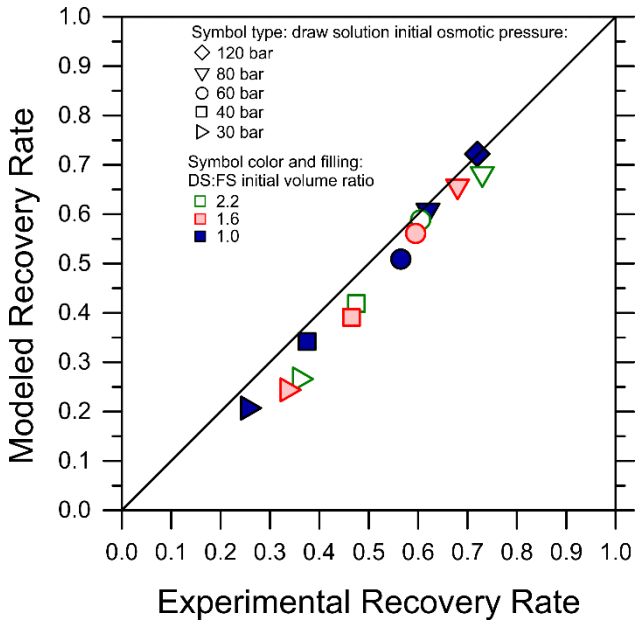

Figure 2: Simulated recovery rates vs. experimentally observed recovery rates for each tested condition of DS initial osmotic pressure and DS-to-FS-initial-volume ratio.

3.2. Observed Productivity of the FO Step and Validation of the Water Flux Simulations

High-recovery tests were conducted with the synthetic PW as FS and $MgCl_2$ solutions as DS using different combinations of DS initial osmotic pressure and DS-to-FS-initial-volume ratios; see Table 2. Figure 3 reports the observed water fluxes as a function of the recovery rate. The continuous lines represent the fluxes predicted with

a forward simulation that combines volume and osmotic pressure balances for each high-recovery experimental condition. Therefore, they are not the result of data fitting, but independent results obtained by applying FO water and solute analytical equations for each time step as a function of the recovery rate. The results are akin to those that would be obtained along a cross-flow membrane module as a function of the recovery rate prevailing in each point of the module. A perfect membrane rejection was assumed for the simulations since no substantial difference in the flux prediction was observed when the rejection was assumed to be as low as 97%. Note that the experimental and simulation results were divided into two graphs with different scales of the ordinate axis, simply for a better visualization of the otherwise large amount of data.

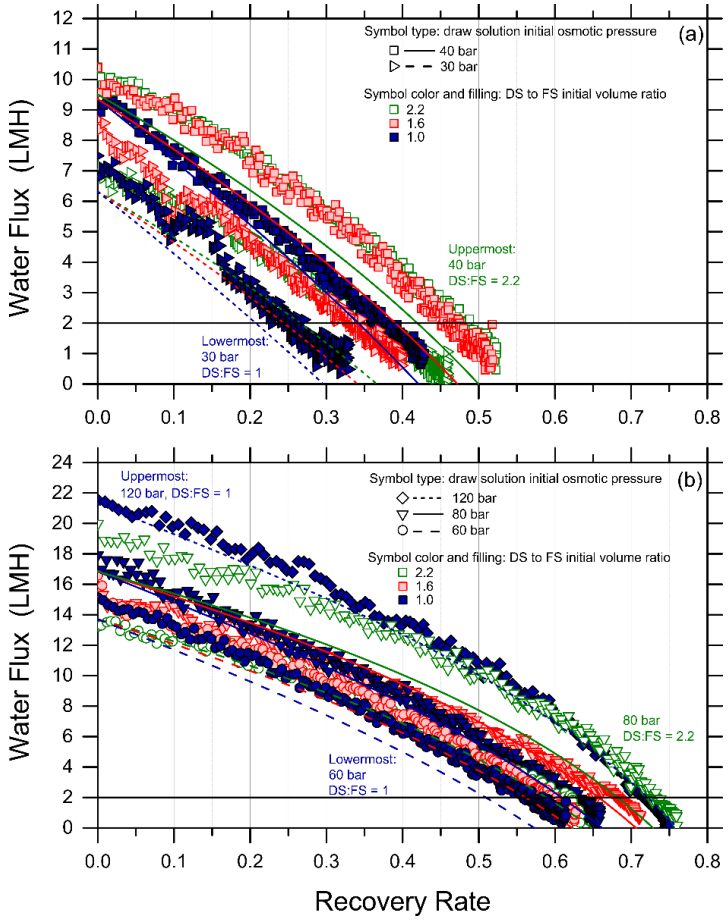

Figure 3: Water fluxes measured (data points) and simulated (lines) in forward osmosis as a function of water recovery rate.

As per figure 3, The initial draw solution bulk osmotic pressures were: 30 bar ((**a**); rightward triangles for the experimental data, continuous lines for the simulated data), 40 bar ((**a**); squares, dash lines), 60 bar ((**b**); circles, dash lines), 80 bar ((**b**); downward triangles, continuous lines), and 120 bar ((**b**); diamonds, dotted lines). The draw-to-feed initial volume ratios were: 1 (solid blue experimental data, blue lines); 1.6 (shaded red experimental data, red lines); and 2.2 (empty green experimental data, green lines). Tests were conducted with a synthetic produced water pretreated effluent as FS (Table 1), at 21 ± 1 °C, with a membrane active area of 23 cm^2, and cross-flow rates of 1.8 L/min in both FS and DS channels. The horizontal black lines at 2 LMH correspond to a hypothetical lower bound of process feasibility in terms of productivity.

As expected, both the experimental and simulated water fluxes showed a decline as a function of the recovery rate, attributed to the reduction in the driving force as water moved from the feed side to the draw side. Average water fluxes spanned from roughly 4 to 10 LMH; see Table 2. Moreover, according to theoretical expectations, the higher the initial DS osmotic pressure and the higher the DS-to-FS-initial-volume ratio, the larger both the measured fluxes and the achieved recovery rates, generally. To assess the feasibility of the technique, the achieved recovery rate values were estimated for each condition at the point where the water flux profile crossed the 2 LMH horizontal black line in Figure 3. This choice was made to be conservative and because lower fluxes may not be considered technically feasible in real operation. Given this assumption, the highest recovery rate of approximately 73% was achieved under two conditions: (i) an initial DS osmotic pressure of 120 bar and a draw-to-feed initial volume ratio of 1 (solid, blue diamonds in Figure 3b), and (ii) an initial DS osmotic pressure of 80 bar and a draw-to-feed initial volume ratio of 2.2 (empty, green,

downward triangles in Figure 3b). The lowest recovery of 25% was observed in the test employing the lowest DS initial osmotic pressure, i.e., 30 bar, and the lowest DS-to-FS-initial-volume ratio of 1. See also Table 2 for a summary of the achieved recovery rate values.

Table 2: Summary of water flux and recovery results in the FO and NF tests.

DS Initial Osmotic Pressure (bar)	DS-to-FS Initial Volume Ratio	Average Experimental FO Water Flux [a] (LMH)	Experimental Recovery Rate @ 2 LMH	Average Experimental NF Water Flux [b] (LMH)	$MgCl_2$ System Rejection
30	1	4.2	25%	26.3	94
30	1.6	4.4	34%	24.0	79.5
30	2.2	4.2	38%	13.3	96.3
40	1	4.9	34%	30.5	90.5
40	1.6	5.3	38%	23.6	93
40	2.2	5.5	41%	21.0	96.6
60	1	6.9	50%	32.3	87.5
60	1.6	7.3	54%	10.9	74.8
60	2.2	6.7	58%	18.6	95.5
80	1	7.9	62%	N.A.	N.A.
80	1.6	7.3	63%	N.A.	N.A.
80	2.2	9.6	65%	N.A.	N.A.
120	1	10.2	73%	N.A.	N.A.

[a] Between the initial value and the value of 2 LMH

[b] Applied feed hydraulic pressure were: 36 bar, 48 bar, and 68 bar, for target final concentrated DS with osmotic pressure of 30 bar, 40 bar, and 60 bar, respectively

N.A.: not available (NF experiment not performed).

While the simulations predicted the initial water fluxes and the trends in an adequate fashion, in a few cases, they underestimated the flux values and the final recovery rate, with a discrepancy compared to the experiments of up to 20%. This discrepancy may be partly due to experimental variation, to a systematic underestimation of the membrane transport performance, or to other phenomena not captured by the simple FO transport equations, but it suggests that fouling did not occur

considerably during the tests and that forward simulations may be used as a conservative means to predict the recovery rate achieved under conditions not explored experimentally. Indeed, when plotting the experimental recovery rate against the simulated recovery rates, the data sit remarkably close to the 45-degree line (see Figure 2). For this purpose, the recovery rates were retrieved as the water flux reached the lowest value of 2 LMH. The color and symbol codes of the data points are consistent with Figure 4. The 45-degree line is also plotted.

3.3. Predicted Productivity of the FO Step

Discussed herein are selected results obtained by one-dimensional, system-wide simulations deploying the analytical FO water flux equation, which was discussed above as adequate and conservative in predicting recovery rates under various scenarios. A first exploration provides insights into the impact of co-current and counter-current configurations. It is important to note that the experiments described above implicitly represent a co-current configuration, as the increasingly concentrated FS are put in contact through the membrane with the increasingly diluted DS. The simulations were stopped when the water fluxes reached a lower limit of 2 LMH. As expected, counter-current configurations were predicted to be characterized by more uniform fluxes as a function of the recovery rate and to consistently yield higher recovery rates; see Figure 4a, which presents the results obtained with a DS-to-FS-influent-flow-rate ratio of 2 and $MgCl_2$ as the draw agent. Specifically, the predicted, achievable recovery rate in the counter-current configuration was between 40% higher, for an influent DS osmotic pressure of 25 bar, and 15% higher, for an influent DS osmotic pressure of 60 bar, than that associated with a co-current configuration, reaching a value of roughly 67.5% for the latter DS influent osmotic pressure. DS

osmotic pressure values larger than 60 bar were considered unfeasible from a practical point of view. As illustrated in Figure 4b, a counter-current configuration does not necessarily provide larger recovery rates when the same membrane area is available in the system, but it allows for the exploiting of a considerably larger membrane area with fluxes larger than 2 LMH compared to a co-current configuration, ultimately resulting in a substantially higher recovery rate for a reasonable investment in terms of the membrane area

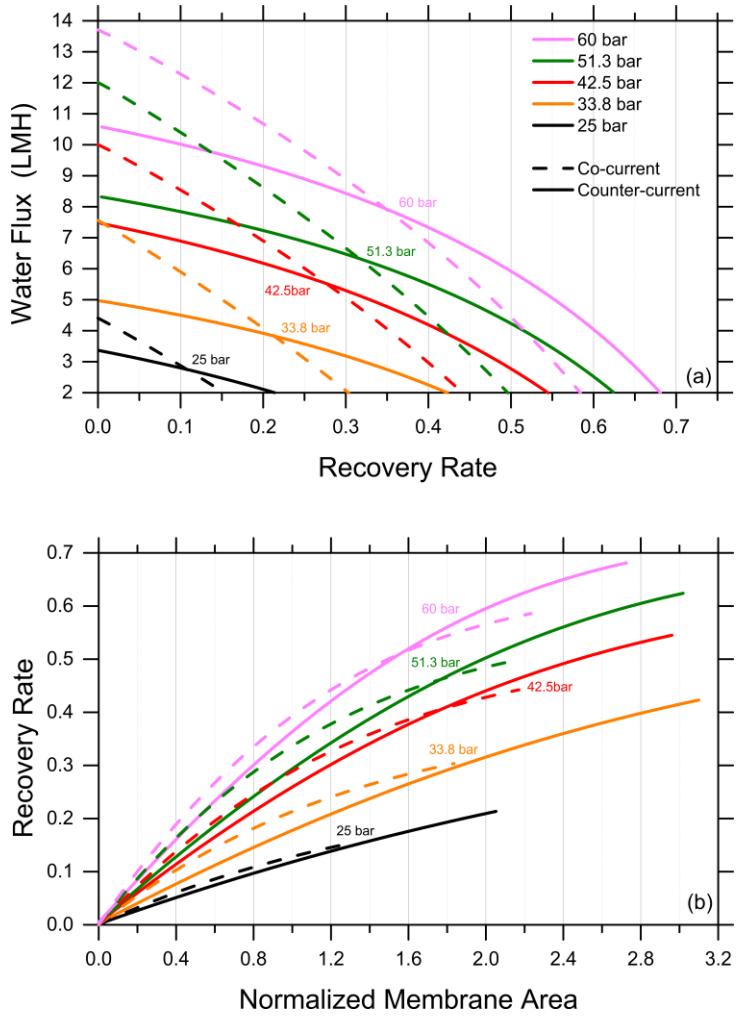

Figure 4: Productivity of an FO system simulated under co-current vs. counter-current configurations.

(a) Water fluxes as a function of recovery rate / (b) Recovery rate as a function of normalized membrane area. Representative results for the case of MgCl2 as draw agent, a DS-to-FS-influent-flow-rate ratio of 2, and stopping the simulations at water flux values equal to 2 LMH. Absolute membrane area depends on the flow rate that requires treatment. Normalization allows comparison among the different conditions for a fixed influent flow rate.

While the selected results plotted in Figure 4 provide a first understanding of the potential range of FO system productivity, Figure 5 presents a more complete set of predictions based on simulations. In particular, a wide range of simulations were performed under the more advantageous counter-current configuration, by varying the DS ($MgCl_2$) influent osmotic pressure and the DS-to-FS-influent-volume ratio. Then, the obtained, achievable recovery rates (up until a water flux of 2 LMH) were simply interpolated to create the color maps illustrated in Figure 5a–c, which would allow the estimation of the (Figure 5a) achievable recovery rate and (Figure 5b) relative exploitable FO membrane area under a wide range of conditions. Note that, because they are the result of the interpolation of discrete results obtained with analytical simulations, these maps are not fully rigorous or analytical. The results suggest that the DS-to-FS-influent-flow-rate ratio would not have an impact on the achievable recovery rate, and the DS influent osmotic pressure governs instead this system response. However, the FO membrane area required to achieve such recovery rates would be lower at high DS:FS influent flow rate ratios, and this mechanism is expected due to the lower DS dilution along the membrane modules. In particular, the map related to the relative FO membrane area illustrates a non-trivial trend, with a maximum for a medium range of the DS influent osmotic pressure and low DS-to-FS-influent-flow-rate ratios. Therefore, an optimization seems possible to maximize the recovery rate and minimize the required FO membrane area.

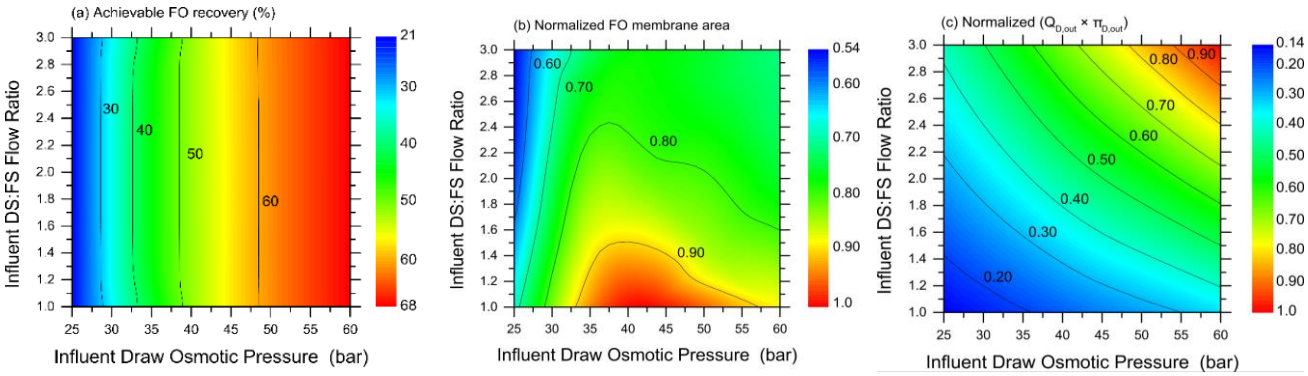

Figure 5: Simulation-based predictions of FO system behavior and productivity in co-current configuration, as a function of DS influent osmotic pressure and DS-to-FS-influent-flow-rate ratio.

(**a**) achievable recovery rate in the FO step; (**b**) relative required FO membrane area (normalized by the highest value in the map); and (**c**) empirical parameter representing the product between effluent DS flow rate ($Q_{D,out}$) and effluent DS osmotic pressure ($\pi_{D,out}$), which provides insight into the complexity/cost of the subsequent draw recovery step. Blue and red colors represent low and high values of the investigated parameter, respectively. Simulations were run with $MgCl_2$ as draw agent and until a water flux equal to 2 LMH was calculated.

Indeed, it would be simple to increase the recovery rate and reduce the required FO membrane area by working at a larger DS influent flow rate and/or a larger DS influent osmotic pressure. However, such conditions may render the subsequent DS regeneration step unfeasible. To obtain a qualitative assessment of the overall complexity of the nanofiltrations step aimed at extracting 100% of the freshwater previously recovered in the FO step and to completely regenerate the DS at the influent values of the osmotic pressure, the fully empirical parameter depicted in Figure 5c was calculated. This parameter is the product between the flow rate of the DS exiting the FO step, which coincides with the feed solution entering the NF step, and the DS osmotic pressure exiting the FO step. In fact, as the two variables increase, larger areas and lower fluxes would be associated with the NF system, with a near equal contribution from the two; see Figure 5c. Overall, the combined plots in Figure 5 provide insight into the most suitable combination of FO conditions that may be technically feasible while translating into a lower full system complexity. Just as an

example, working with a DS influent osmotic pressure of about 52.5 bar and at a DS-to-FS-influent-flow ratio of 1.4 seems to allow the achievement of a recovery rate of approximately 62% with average water fluxes of 6.0 LMH, reasonably low FO membrane areas, and limiting the complexity of the NF step, the latter being the subject of the next chapter.

3.4. Draw Solution Regeneration and Freshwater Extraction with Nanofiltration

Water fluxes measured in the nanofiltration tests are reported in Figure 6. The diluted draw solutions from nine FO experiments were regenerated in NF, corresponding to DS initial osmotic pressures in FO (coinciding with target osmotic pressure upon NF reconcentration) of 30, 40, and 60 bar and draw-to-feed initial volume ratios of 1, 1.6, and 2.2 (each pressure tested at three different ratios). The applied pressures in the NF experiments were 36, 48, and 68 bar, respectively, for the three target osmotic pressure values. In this work, no obvious damage was observed for any of the NF membranes. However, note that commercial NF membrane modules have a maximum pressure rating that may be lower than the pressure values applied in this study. As expected, due to the increasingly high osmotic pressure of the concentrate solutions along the tests, Figure 6a shows that the water flux decreased with the increasing relative recovery rate. Water fluxes spanned from roughly 10 to 33 LMH, substantially higher than those observed in the FO step. A 100% relative recovery rate was obtained in all the NF tests. Note that the trends observed in NF were not as neat as those measured in FO. Moreover, the experimental data were predicted only in a broad way by the forward simulations performed using the NF analytical water flux equation. The discrepancies may be due to an instability of the NF system

and/or of the NF membrane at high applied pressure, which ranged between 36 and 68 bar.

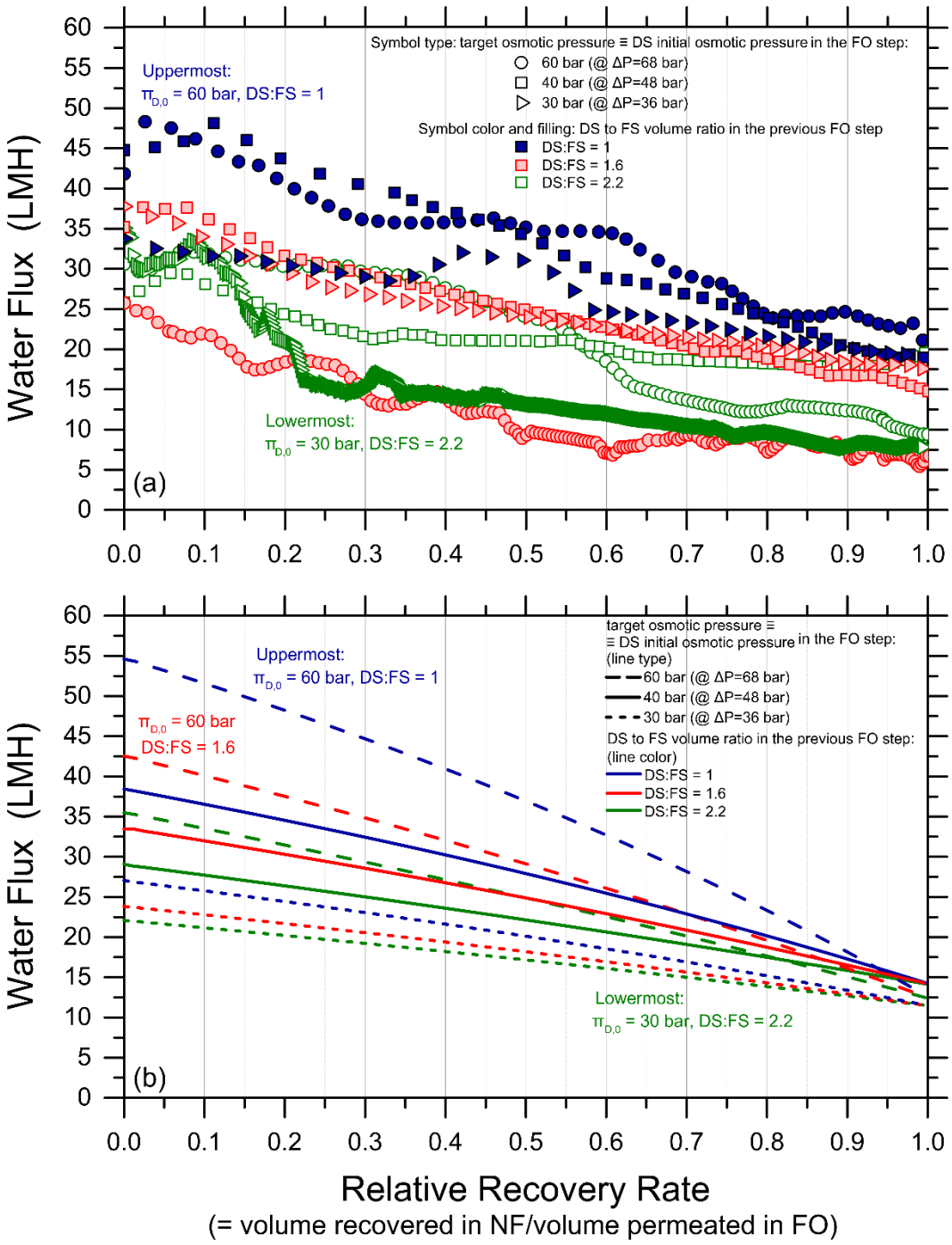

Figure 6: Water fluxes in nanofiltration as a function of relative recovery rate

The relative recovery rate is calculated as the ratio of the volume of water recovered in nanofiltration (NF) to the volume previously permeated in forward osmosis (FO). (**a**) Experimental data and (**b**) results of simulation using the NF analytical water flux equation taking into account concentration polarization by applying a feed channel mass transfer coefficient of Commercial NF90 membranes, were used (Dupont). The applied pressure was in the range of 36–68 bar depending on the initial osmotic pressure of the synthesized draw solution. In (**a**), circles, squares, and triangles refer to DS that needed to be regenerated to 60 bar, 40 bar, and 30 bar, respectively. Blue, red, and green colors refer to diluted DS obtained in previous FO experiments with DS to FS initial volume ratios equal to 1, 1.6, and 2.2, respectively.

3.5. Quality of the Product Water

An analysis of the composition of all streams entering and exiting the FO and NF units was conducted. The majority of cations and metals exhibited a medium to high retention by the FO membrane. Specifically, the observed rejection was 97.5% for Na, 66.3% for B, 99.3% for Ca, and 94.8% for K, on average. Additionally, the acetate and sulfate concentration in the draw side were under the detection limit, indicating a near-total retention by the membrane. No substantial increase in magnesium or chloride was observed in the feed solution, suggesting a limited reverse solute flux occurring during the tests. When considering the nanofiltration step, the average retention of Mg and Cl by the NF membrane was 93% and 81.9%, respectively. Table 3 shows the characteristics of the final product water obtained through the nanofiltration treatment of the diluted DS coming from the high-recovery experiments. The TOC content was low, corroborating that the FO-NF double barrier prevented the passage of acetate. However, the total dissolved solids (TDSs) concentration of the

final product water, coinciding with the nanofiltration permeate stream, was in the range of mildly brackish water and also contained a certain amount of sodium. These results suggest that the FO-NF double barrier allows the non-negligible passage of monovalent ions and, more importantly, that nanofiltration membranes may not be sufficiently dense to retain the DS at a sufficient rate. Similar conclusions may be drawn by analyzing the data in terms of $MgCl_2$ regeneration. The so-called "$MgCl_2$ system rejection" presented in Table 2 was calculated as the draw solute concentration in the final volume of the extracted freshwater divided by the $MgCl_2$ concentration in the initial DS used for the relative FO experiment. The highest system rejection was 96.6%. Note that, in most tests, the overall FO-NF system rejection lay between 90 and 96%, but, in two cases, it was considerably lower than expectations. The low rejection values may be due to experimental issues, including a non-optimal membrane sample and/or errors in the water analysis, and should not be considered reflective of the expected behavior of a perfectly functioning system in the opinion of the authors. Overall, the results suggest that, while a complete recovery of the freshwater could be achieved, a non-negligible fraction of the draw agent would be lost throughout the system, mostly due to the incomplete rejection in the NF step, but also partly due to scaling and through losses as a reverse solute flux in FO. Practically, in order to maintain the target osmotic pressure, 5–10% of the initial agent would need to be consistently added to the recirculated draw stream. As discussed also by previous studies, such losses may, in some cases, represent an important limitation, resulting in the impaired technical and economic feasibility of the combined system [61,68–70]. In this sense, RO membranes may be necessary for the correct regeneration of $MgCl_2$ or other similar solutes, which would lower the productivity of this second system step

and require larger membrane areas than those that would be associated with a nanofiltration unit [71,72].

Table 3: Composition of the final product water from combined FO and NF filtration tests.

DS Initial Osmotic Pressure (bar)	DS-to-FS Initial Volume Ratio	TOC (ppm)	Na (ppm)	Mg (ppm)	Cl^- (ppm)	B (ppm)	TDS (ppm)
30	1	2.3	137	344	882	<0.3	~1360
30	1.6	4.2	168	1560	3300	<0.3	~5030
30	2.2	1.3	245	288	800	<0.3	~1330
40	1	1.5	93	773	1420	<0.3	~2290
40	1.6	1.7	160	669	1520	<0.3	~2350
40	2.2	1.1	94	723	1490	<0.3	~2310
60	1	3.9	210	1270	2630	<0.3	~4110
60	1.6	2.4	134	1300	2700	<0.3	~4130
60	2.2	1.2	153	480	1150	<0.3	~1780

4. Conclusion

The aim of the current study is to provide insight into the technical feasibility of a system comprising forward osmosis and nanofiltration for the extraction of freshwater from a synthetic produced water with an osmotic pressure of 16.3 bar, representative of a mix from upstream fossil fuel extraction activities and of minor condensates and water flows originated in the separation processes of hydrocarbons. High-recovery FO tests were performed using $MgCl_2$ as the draw agent at varying values of the draw solution osmotic pressure and draw-to-feed volume ratios. The results of the simulations based on the FO transport equations were thus validated, and then applied to predict the recovery rates achievable under a wider range of operating conditions. High-recovery NF tests and simulations were finally performed to describe the ability in extracting freshwater and regenerating the DS. Note that this study has some

limitations, among which are the use of a synthetic feed solution, and the limited duration of the experiments that did not allow an appraisal of the fouling behavior. That being said, the tests conducted at high recovery, supported by validated simulations, provide important insight into the technical feasibility of the system for this specific treatment case, but also for a wide variety of applications targeting feed solutions in the same osmotic pressure range.

A combination of forward osmosis and nanofiltration would allow the production of brackish water in the low-salinity range, starting from a produced water with an osmotic pressure of roughly 16 bar (salinity of approximately 20 g/L) and at recovery rates between 55 and 65% (if working under the counter-current configuration in the FO step). Based on both experimental and modeling results, the overall system would have important drawbacks. One drawback is the inability to produce freshwater at a salinity lower than 500 mg/L. Another limitation, already pointed out by previous studies, would be the low productivity in the FO step, with average fluxes in the order of 6 to 8 LMH with the influent $MgCl_2$ draw solution characterized by an osmotic pressure of around 50 bar. This high osmotic pressure, combined with the imperfect rejection rate of the solute in nanofiltration, implies the need for the substantial replenishment of the draw agent at each recirculation (5–10% in mass). The system may thus require the use of highly dense RO membranes in the second step, even with a 2:1 draw agent such as $MgCl_2$. With RO membranes and at a similar or only marginally higher applied pressure with respect to those associated with NF membranes, a higher draw agent rejection would be achieved at the expense of some loss in the water flux, but still maintaining average productivities that are likely substantially higher than those associated with the first FO step. Overall, while the first

(FO) step seems to be the limiting factor in terms of the water productivity [63], the second (NF or RO) step seems, instead, to be the limiting factor in terms of the ability of saving the draw agent and producing a high-quality final water product, when the membranes are not highly dense. Attempting a rational evaluation of the technical feasibility of the FO-based system under similar conditions, this study suggests, along with several recent investigations on the feasibility of forward osmosis, that this technique is likely suitable for applications entailing the dilution or the concentration of high-value solutions and/or when an inexpensive draw agent or draw solution is widely available. Applications aiming at extracting high-quality freshwater from streams of medium or high salinity may be feasible at medium to high costs, with the materials (e.g., membrane, and draw agents) that are available today. Any detrimental effects, such as fouling or membrane deterioration, or other requirements, such as membrane cleaning, chemical additions, and pre- or post-treatment, none of which were investigated in this study, would add potential further complexity to the system. The complexity and variability of the real produced water could add further issues. Note that the scope of this study does not include any economic or environmental considerations, which would be necessary to make a final, informed decision on the applicability of the technique.

Chapter 2: Technical Feasibility of the Concentration of Amine Water using Forward Osmosis[2]

1. Introduction

Raw natural gas exists in nature among other components within deep underground reservoirs. After the extraction of natural gas to the surface, it must be processed to remove impurities until levels acceptable to final users [74,75]. Among these impurities are hydrogen sulfide H_2S and carbon dioxide CO_2, which can cause corrosion and other major safety risks. H_2S is poisonous even at low concentrations and need to be properly disposed before natural gas is transported or commercially distributed. Among the methods of H_2S and CO_2 removal from natural gas (sweetening) is the use of aminated compounds. These compounds have been also considered for carbon capture processes [74,76-79].

The reduction of the H_2S content in the raw natural gas is usually carried out by scrubbing with aqueous solutions of tertiary alkanolamines (e.g., N-methyldiethanolamine, MDEA) inducing the formation of the respective salts. The latter ones are subsequently thermally decomposed allowing the recycling of the scrubbing solutions and at the same time the liberation of a gaseous stream enriched into hydrogen sulfide (e.g., to be sent to a Claus reactor). The periodic replacement (partial or total) of the aqueous solutions of tertiary alkanolamines is necessary due to their progressive deterioration as the scrubbing and regeneration cycles follow. The resulting liquid waste (hereinafter referred to as "amine water") has a pH greater than

[2] The contents of this chapter are part of a patent application submitted on January 2023 with patent disclosure nr. H23013 under the name “Procedimento Per La Concentrazione Di Acqua Amminica A Temperature Ambiente”.

12.0 and high contents of both organic and inorganic compounds due to degradation of amine reagents (e.g., ammonia, corrosion byproducts, heat-stable salts, and other degradation products). Natural gas plants can face many challenges dealing with these amine water streams: for example, (i) corrosion of metal can occur and cause damage to pipelines / components; (ii) accumulation of organic acids due to foaming (from interaction between natural gas and amines); (iii) vaporization and solvent loss at high temperature when the amines are characterized by high vapor pressure; (iv) accidental release of leachate to the environment, affecting aquatic life. These phenomena make the handling and the treatment of amine waters difficult, thus they increase maintenance and operational costs [80,81]. The amine water is usually sent to pyrolysis [82]. The latter one has some drawbacks. Firstly, it involves prohibitive costs, especially if its transport is necessary (e.g., by tankers). Secondly, it involves elevated temperature degradation, which requires a considerable amount of energy that could be utilized elsewhere. Fourthly, pyrolysis exhaust gases contain high concentrations of CO_2, which require further treatment before it can be vented [82-88]. Transport issues are more important as the volume of amine water that needs treatment is higher. In this sense, reducing the volume of the stream by dewatering translates into economic and logistical benefits. As a result, there is an increasing demand for innovative wastewater management strategies [89-92].

Amine water discharge in landfills is thereby prohibited. Moreover, amine water cannot be efficiently biodegraded due to its low C/N (carbon: nitrogen) ratio, and all processes based on biodegradation require large reactor volumes and treatment times. Distillation, for example, is expensive in terms of energy requirements, while established membrane processes cannot be applied due to high risks of fouling and

scaling. Also, the typically high pH of these techniques significantly impairs them by inhibiting biochemical reactions or because the materials used to construct the components are not compatible with highly alkaline environments, e.g., they get corroded [74, 91-96].

The aim of this study is the concentration of amine water by dewatering using forward osmosis at ambient temperature and atmospheric pressure. The membranes used are made of polyamide, polysulfone, and/or polyester, similar to reverse osmosis membranes, thus obtained from highly consolidated manufacturing procedures. The equipment does not require special materials capable of withstanding the chemical aggressiveness of amine water. From this point of view, forward osmosis has shown promising results for amine water treatment.

2. Literature and Patent Review

EP 0,918,049 A1 (27 October 1997, Shell International Research Maatschappij) describes a process of treating amine water by distillation. The process includes at least two successive steps: in the first there is dehydration while in the second there is the purification of the alkanolamine. Examples are: the treatment of an amine water containing 42% wt. diisopropanolamine, 55% wt. of water, residual degradation products (it operates at 154-177 °C by applying vacuum); the treatment of amine water containing 40% wt. of methyldiethanolamine, 29% wt. of water, 31% wt. of sulfolane, the rest of degradation products (it is operated at 135 - 148 ° C by applying vacuum). [97]

Concentration by nanofiltration or reverse osmosis requires the application of high hydraulic pressures (from 5 to 150 bar) and is subject to membrane fouling. For this reason, these systems are proposed downstream of pretreatment processes. [98]

US 9,028,654 B2 (29 February 2012, Alstom Technology) describes an amine water treatment process comprising two evaporative processes and a reverse osmosis process. Water with a purity greater than 95 - 99% wt. is obtained. [99]

US 5,171,499 (6 June 1992, Texaco) describes a process of treatment of amine water by means of pervaporation. The process is based on composite membranes consisting of a layer of dense polyvinyl alcohol deposited on a porous alumina support. The porous alumina support is necessary to ensure chemical resistance to the amine. The dehydration of mixtures 74 - 78% wt. is exemplified. of amine, water rest (experiment is operated at 70 ° C by applying vacuum in the distillate sector). Selectivity of water in the distillate of 57 - 60% and distillate flow of 3.1 - 1.6 kg / (m^2.h) are obtained. The membrane is stable for 22 days. [100]

US 5,334,314 (December 3, 1990, Deutsche Carbone) describes a process of treatment of amine waters by means of pervaporation. Acid-treated polyvinyl alcohol membranes are used. The dehydration of a mixture containing 70% wt. is exemplified. % ethylamine, 30% water (it is operated at 85 ° C; a distillate flow of 0.750 kg / m^2.h is obtained). Also exemplified are: the dehydration of a mixture containing 40% wt. of pyridine, 60% wt. of water (it is operated at 95 ° C); the dehydration of a mixture containing 70% dimethylamine and 30% wt. of water (it is operated at 100 ° C); the stability of the membrane at temperatures close to 100 ° C and high concentrations of

amine. In all the examples cited, one presumably operates by applying vacuum in the distillate sector.[101]

US 5,051,188 (31 October 1990, Basf Aktiengesellschaft) describes a process of treatment of amine waters by means of pervaporation. Polyvinyl alcohol membranes are used. Water is removed from mixtures that contain it together with carbon dioxide and amine mixtures. The dehydration of a mixture containing 45% wt. is exemplified. of methylamine (as such or as carbamate), 28% wt. of carbon dioxide, 27% wt. of water (it is operated at 80 ° C by applying a vacuum in the distillate sector). A distillate flow of 0.500 kg / m2 * h is obtained.[102]

JP 1998137786 (May 26, 1998) describes a process of treating amine water such as water-soluble cutting oil containing liquid waste. The pH of the amine water is adjusted. Then, the water is sent to biological treatment using microorganisms to decompose the amine. The water was circulated between the tank for pH control and that for biological amine decomposition until the desired amine concentration is achieved. [103]

JP 2010131489 (June 17, 2008) describes a process of treating aromatic amines water through an extraction treatment using an aromatic hydrocarbon solvent. The extraction is performed in a pH 5-8 and temperature of 60-80 ^{o}C to separate oil and water. The obtained aromatic amine is recycled to the extraction treatment. The chemical oxygen demand (COD) of the aromatic amine wastewater of about 2500-5000 ppm. After the above treatment, the COD decreased to 1000-700 ppm. [104]

KR 1020130095038 (August 27, 2013) describes a process of treating nitrogen-rich water in three main steps. Firstly, conversion of amines and organic matters into

ammonia using microorganism in a biological reactor. Secondly, ammonia stripping in an aeration tank. Finally, the remaining dissolved organic matter is digested with microorganism in a second biological reactor. [105]

US 20190263685 (August 29, 2019) describes a forward osmosis system for treating saturated brine in an oil and/or gas treatment facility. The feed side is water containing cations, anions, carbonate, and bicarbonate obtained from a source of produced water associated with oil and/or gas production. The draw side contains a saturated brine solution. Water passes from the feed side to the draw side diluting the brine draw while concentrating the produced water. The proposed system discloses the dilution of the saturated brine without the direct addition of soft water. The effectiveness in the treatment of amine waters is not exemplified. [106]

CN 107413196 (December 1, 2017) describes the method of synthesizing a forward osmosis membrane to be used for the treatment of pesticide-rich water. Firstly, the membrane support layer is prepared by adding water, attapulgite, and acetyl trimethyl ammonium bromide while subjecting the mixture to ultrasonic treatment. Secondly, ethyl alcohol and mercaptopropyltrimethoxysilane were added in sequence. Thirdly, pesticide-rich water is treated by circulating the water in the forward osmosis device using the prepared forward osmosis membrane. Finally, further treatment was applied using reverse osmosis membrane to obtain pure water. The effectiveness in the treatment of amine water is not exemplified. [107]

WO 2012106732 (August 9, 2012) describes the process of concentrating methane digester effluent for fertilizer production using forward osmosis system. The system includes a digester stage coupled with a coarse filtering stage to produce a

residual water stream. Acid treatment is applied afterwards to retain ammonium in the water. This ammonium-rich water is used as the feed solution while a saturated salt brine stream is used as the draw solution in the forward osmosis system. Due to the concentration gradient between the two solutions, the brine stream is diluted while the ammonium-rich water is concentrated, producing a fertilizer stream. [108]

WO 2020056508 (March 26, 2020) describes the methods of manufacturing forward osmosis (FO) and membrane distillation (MD) membranes to be used for the treatment of fracking water. The FO membrane is composed of a microporous electrospun nanofibers support layer and a hydrophilic nanocomposite rejection layer. The MD membrane is a microporous electrospun nanofibers mat developed from a nanocomposite with dispersed graphene oxide. Fracking water is subjected to microfiltration as a pre-treatment step. Then, the pre-treated water is used as the feed solution against a high salinity draw solution in the FO system. Finally, the diluted draw is treated using MD to produce water and regenerate the draw solution. The effectiveness in the treatment of amine water is not exemplified. [109]

US20220204375 (June 30, 2022) describes a water treatment system that has a forward osmosis liquid concentration and an electrodialysis (ED) apparatuses. When treated in the FO liquid concentration apparatus, the concentration of salts in the water increases between 7% to 14%. Then, the concentrated water stream is received by the ED apparatus to convert the salt in the water into an acid solution and a base solution. Finally, the remaining aqueous solution is mixed with the untreated water and the mixture is fed to the FO apparatus again. The above steps are repeated until zero discharge is achieved. The effectiveness in the treatment of amine waters is not exemplified. [110]

Oh et al. investigated the efficiency of combining advanced oxidation processes (AOPs) and biological treatment process (BWTP) for the treatment of water produced in the steel-making industry. This water is rich in MDEA with a concentration up to 20,548 mg/L including some other organic contaminants such as formate, phenol, and thiocyanate. Three different AOPs (i.e., Fenton, ozone, and peroxone) were tested as a pre-treatment step and the peroxone method, using ozone and H_2O_2, showed the highest selectivity, 92.87%, for MDEA degradation. Respirometer tests performed on the BWTP sludge showed that the microbial toxicity of the peroxone-pretreated water is negligible. Furthermore, the biochemical oxygen demand (BOD) to COD ratio showed a significant increase in the biodegradability of wastewater from 0.103 to 0.147 as a result of the peroxone pretreatment. The oxygen uptake rate analysis revealed that the contaminates microbial degradation rate was in the order of phenol > formate > thiocyanate > MDEA. [111]

Furhacker et al. used aerobic treatment process to investigate the biodegradability of MDEA-rich water. The 40% MDEA-rich water was obtained from a gas sweetening plant and two main tests were performed: a batch test and a continuous flow one (40 L/d). The batch test results showed that in a period of 28 d, MDEA did not show any sign of degradation. However, the TOC measurements of the continuous flow experiments revealed that 96% of the MDEA was biodegraded by adapted microorganisms. [112]

Campo et al. studied the aerobic biodegradation of different amines in two saline water samples with NaCl concentration of 3% and 7%. A mixture of aliphatic amines (e.g., N-(2- aminoethyl) ethanolamine (AEA), N,N-diethylethanolamine (DEA), N,N-bis(2-hydroxyethyl)methylamine (MDEA), tris(2-hydroxyethyl)amine

(TEA), and cyclohexylamine (CHA)), and primary aromatic amines (e.g., aniline (ANL), 4,4'-methylenedianiline (4,4'-MDA)) were present in both samples. The biodegradation rate of TEA and MDEA did not show any dependence on the salinity, while AEA and DEA rate increased in 3% NaCl. CHA did not show any degradation in 7% NaCl. However, in 3% NaCl, total degradation happened. 40 % ANL was degraded in 24 h period, and full degradation was observed after 48 h. 4,4'–MDA remained intact in 7% NaCl. However, it was fully degraded in 3% NaCl. [113]

Libralato et al. tested the removal efficiency of ethanolamine and other organic pollutants from industrial oily water using a sequence of evaporation and air-stripping processes. After a chemical breaking procedure, a vacuum evaporation was applied, using a lab-scale plant, at three different temperatures (T= 50, 70, and 80 °C). The laboratory results showed that at T= 50 °C, the condensate phases were efficiently removed. At higher temperatures, ammonia and organic compounds were considerably removed (>97% for COD) along with the toxicants reduction (>95% for Toxic Unit at 50%). Furthermore, a full-size water treatment plant (WWTP) was used to also evaluate the competence of the evaporation processes on a real scale. The role of monoethanolamine (MEA), diethanolamine (DEA), and triethanolamine (TEA) in toxicity definition was investigated after the air-stripping process. A reduction in ammonia concentration was achieved for both ionized and unionized ammonia. In addition, an increase in toxicity was measured from TEA to DEA to MEA. [114]

The effect of thermal degradation on monoethanolamine (MEA) and its removal capacity of CO_2 was investigated by Zoannou et al. MEA samples were exposed to elevated temperature (160 °C) from 2 to 8 weeks while measuring the decline in their CO_2 removal capacity. After 8 weeks of thermal treatment, MEA

concentration declined by 85% and 95% for samples with initial molar loading of 0.19 and 0.37 mol of CO_2/mol of MEA, respectively. The remaining solvent retained a CO_2 removal capacity of 22% indicating that the initial CO2 loading did not have an effect on amine degradation. On the other hand, thermal treatment for 2 and 3 weeks showed a dependence on the initial molar CO_2 loading. In addition, the thermal degradation rig revealed high corrosion potential during experimentation with a calculated rate of 1.95 mm/y. [115]

3. Materials and methods

3.1. Membranes and Chemicals

The membranes used for the experiments are polyamide thin film composite (TFC) FO membranes. Following the protocol reported previously by Tiraferri et al. (2013), membrane characterization was performed to determine the active layer water permeance, A, NaCl permeability coefficient, B, and the support layer structural parameter, S, using NaCl as a draw solute and deionized water as the feed solution [66]. The values obtained are 2.74 ± 0.50 L $m^{-2}h^{-1}bar^{-1}$, 0.94 ± 0.25 L $m^{-2}h^{-1}$, and 427 ± 19 μm, respectively.

For the preparation of the amine water feed solution and of the draw solutions, N-methyl diethanolamine (MEDA) (Purity ≥ 99 %, density 1.038 g/mL at 25 ºC) was purchased from Sigma-Aldrich. Triethylene glycol (Purity ≥ 98 %, density 1.12 g/mL at 20 ºC) was purchased from Carlo Erba. Boric acid (H_3BO_3) (molecular weight 61.83 g/mol) and sodium chloride (NaCl) (molecular weight 58.44 g/mol, purity ≥ 99.8%, density 2.165 g/mL at 25 ºC) were purchased from Carlo Erba. Sodium hydroxide (NaOH) (Purity ≥ 97 %, molecular weight 39.99 g/mol)) used for adjusting the feed

solution pH was purchased from Carlo Erba as well. DI water from a Milli-Q (Millipore) system was used in all preparations.

3.2 Feed solution characteristics

Table 4 presents the main characteristics of the feed solution. The PH of the solution was adjusted from 12 to 5 to strip sulfides that exist in the natural amine water.

Table 4: Characteristics of the synthetic amine water used as feed solution

Parameter	Concentration
Organic carbon (ppm)	59063
pH	5
Conductivity (microS/cm)	14500
N-methyldiethanolamine (ppm)	100000
Triethylene glycol (ppm)	3000
Cl^- (ppm)	3000
$B(OH)_3$ (ppm)	50

3.3 Lab-scale membrane filtration setup

The FO experiments were performed using the same system described in the previous chapter. Both the feed and the draw were recirculated back to their reservoirs while water continuously permeates from the feed to the draw stream.

3.4 FO tests

The same protocol was applied for all the experiments. Prior to each experiment, a new membrane was immersed in water (DI for 15 min and then inserted in the cell unit in an FO mode). In other words, the membrane active layer faced the feed solution while the support layer faced the draw solution. Next, 1 L feed solution, pH= 5 and conductivity=14500 µs/cm, and 1 L DI water were added in the feed and the draw tanks, respectively.

The test was carried out as follows: 2.5 L of feed solution was prepared as previously explained and added to the feed reservoir. The draw solution osmotic pressure and/or volume were varied for each experiment. The osmotic pressure values tested were 55, 80, 130, and 140 bars while the volume values were 3.5 L, 5 L, and 6 L. A computer-interfaced balance was used to calculate water flux across the membrane based on the change of the draw solution volume verses time during all the experiments that lasted for almost 24 h each. During that time, the feed and draw solutions were recirculated back to the reservoirs. Generally, the driving force for the FO phenomenon is the difference in osmotic pressures of the feed and draw solutions across the membrane. During the FO process, water molecules permeate from the feed side to the draw side while solute molecules are rejected by the membrane and consequently, the feed solution is concentrated, and the draw solution is diluted. Due to concentration polarization (CP), the osmotic pressure of the feed is increased at the same time the osmotic pressure of the draw is decreased at the active layer of the membrane. In other words, the bulk osmotic pressure difference will be significantly higher than the effective osmotic pressure difference as a result of CP effect. External concentration polarization (ECP) and internal concentration polarization (ICP) are two types of CP that induce the reduction of the effective osmotic pressure difference in FO desalination process. As a result of water transport from the feed to the draw, concentrative ECP happens due to the buildup of solutes on the active layer of the membrane which increases the concentration of the feed at the membrane active layer. Eventually, the water flux declines gradually due to the gradual decrease in the net osmotic driving force. Another major factor for flux decline is attributed to dilutive

ICP. Dilutive ICP occurs as the draw solute within the porous support layer is diluted by the constant transport of water from the feed to the draw.

The recovery rate from the FO tests, *REC*, was calculated as follows:

$$REC = 1 - \frac{V_{P,tot}}{V_{F,0}}$$

where *V* is the volume of a certain solution, the subscript "*P,tot*" refers to the total permeated volume throughout the test that diluted the draw solution, the subscript "*F,0*" to the initial feed volume at the beginning of the test. The concentration factor, *CF*, relates to the recovery rate as:

$$CF = \frac{1}{1 - REC}$$

The so-called "system rejection" of a species is instead calculated as:

$$R = 1 - \frac{c_{D,fin}}{c_{F,0}}$$

and it takes thus into account the concentration of species in the final draw solution volume with respect to the initial concentration in the feed solution at the beginning of the test.

4. Results and Discussion

4.1 Choice of the draw solute and operating conditions

Synthetic amine water was used as the feed solution in a series of preliminary FO experiments to assess the selection of the draw agent and operational parameters for the high-recovery experiments. $MgCl_2$, NaCl, and $C_3H_5NaO_2$, are the draw solutions evaluated in these tests. Figure 7 (a) represents the obtained water flux as a

function of DS concentration while Figure 7 (b) shows NaCl and $MgCl_2$ analytical FO water flux model when used as DS. The models are presented graphically as continuous lines, with no inclusion of extra fitting other than membrane transport parameters, *A*, *B*, and *S*. In addition, taking into consideration the crossflow channel mass transfer coefficient, which remained consistent at 40 LMH for the forward osmosis cell under the crossflow conditions employed during the experiments. NaCl demonstrated the highest fluxes probably as a result of its high diffusion coefficient. This in return decreased the dilutive internal concentration polarization with respect to other compounds. Following NaCl, sodium propanoate showed the second highest fluxes, and finally $MgCl_2$. It is noteworthy that the value of FS bulk osmotic pressure was equivalent to the value of DS bulk osmotic pressure (~30 bar) at which the modeled fluxes went to zero, this was confirmed by these initial tests. Ultimately, NaCl was chosen as DS for the high recovery experiments due to its high flux, abundancy, and cost efficiency.

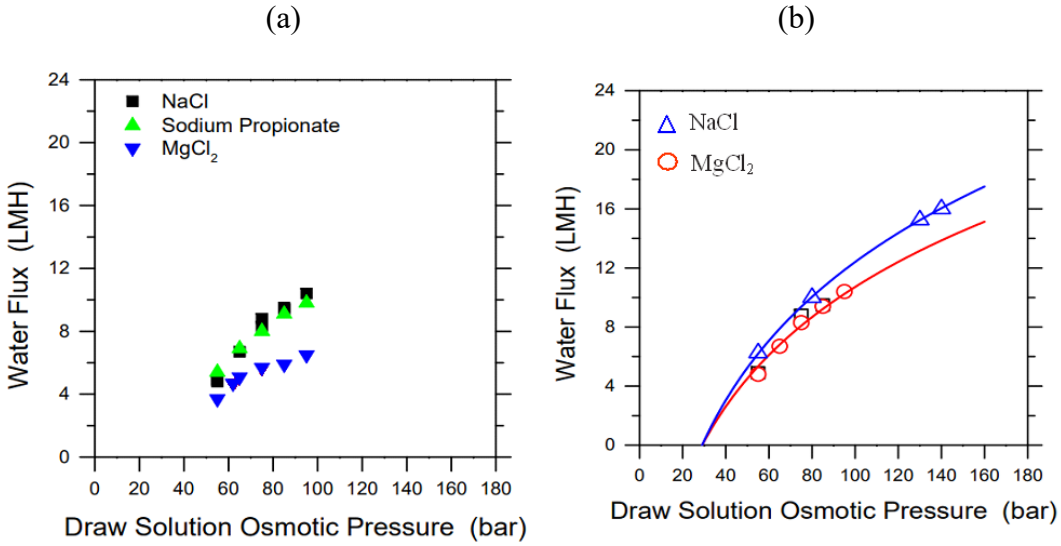

Figure 7: (a) obtained water flux as a function of DS concentration / (b) NaCl and MgCl2 analytical FO water flux model when used as DS.

(a) Fluxes measured in forward osmosis as a function of draw solution osmotic pressure. The feed solution was synthetic amine water. Black, green, red, and blue points represent experimental data obtained with NaCl, $C_3H_5NaO_2$, or $MgCl_2$ as draw agents, respectively. (b) FO analytical water flux model represented as blue and red continuous lines for NaCl and $MgCl_2$, respectively. The model is calculated using the membrane characteristics, a channel mass transfer coefficient of 40 LMH, and the diffusion coefficient of NaCl, and $MgCl_2$, respectively, at 21 °C.

4.2 Observed productivity of the FO step and validation of the water flux simulations.

Utilizing synthetic amine water as FS and NaCl solutions as DS, the high recovery tests were performed by means of different combinations of initial DS osmotic pressure and DS to FS volume ratios; see Table 5. Figure 8 reports the fluxes as a function of the recovery rate. The continuous lines show the fluxes forecasted through a forward simulation, which integrates volume and osmotic pressure balances for every high recovery experimental setting, thus they are not the result of data fitting. The assumptions applied for the simulation of amine water high recovery experiments were similar to that of PW high recovery experiments in the previous chapter.

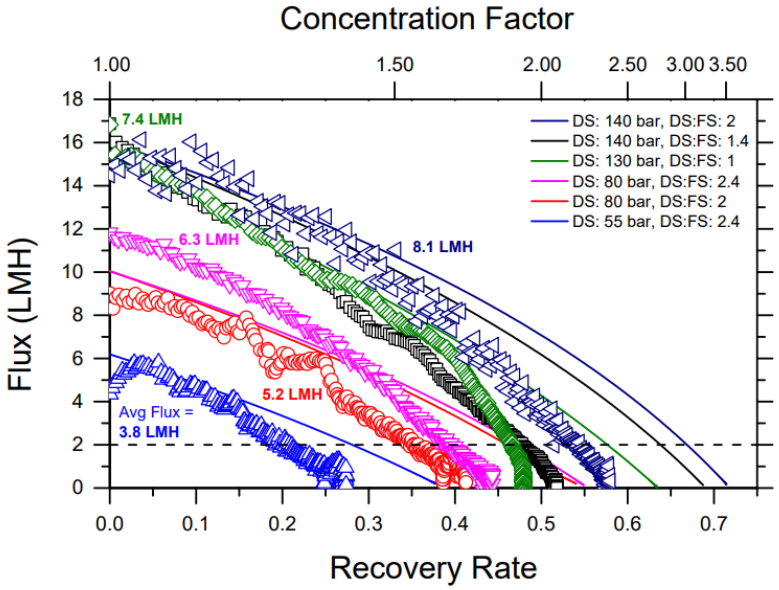

Figure 8: Water fluxes measured (data points) and simulated (lines) in forward osmosis as a function of water recovery rate.

The initial draw solution bulk osmotic pressures were 55 bar (upward triangles for the experimental data, continuous line for the simulated data); 80 bar (circles, continuous line); 80 bar (rightward triangles, continuous line); 130 bar (squares, continuous line); 140 bar (squares, continuous line); 140 bar (upward triangles, continuous line). The draw-to-feed initial volume ratios were: 2.4 (blue experimental data, blue lines); 2 (red experimental data, red lines); 2.4 (Pink experimental data, Pink lines); 1 (green experimental data, green lines); 1.4 (black experimental data, black lines); 2 (navy blue experimental data, navy blue lines); Tests were conducted with a synthetic amine water as Table 4, at 21 ± 1 °C, with a membrane active area of 140 cm^2, and cross-flow rates of 1.8 L/min in both FS and DS channels. The horizontal black lines at 2 LMH correspond to a hypothetical lower bound of process feasibility in terms of productivity.

As anticipated, both the experimental and simulated water fluxes demonstrated an inverse relation with the recovery rate, which can be attributed to the decrease in the driving force as water moved from the feed side to the draw side. Average water fluxes spanned roughly from 4 to 8 LMH; see Table 5. Moreover, theoretically, the higher the initial DS osmotic pressure and the higher the initial DS to FS volume ratio, the larger were both the measured fluxes and the achieved recovery rates. To evaluate the viability of the technique, the acquired recovery rate values were estimated for each condition above the 2 LMH horizontal dashed line in Figure 8. This decision was made for practicality, as lower fluxes may not be technically feasible in real operation. The highest recovery was 55%, achieved by using an initial DS osmotic pressure of 140 and a draw-to-feed volume ratio of 2 (navy blue line in Figure 7). The lowest recovery of 22% was observed in the test employing the lowest DS initial osmotic pressure and DS to FS volume ration, i.e., 55 bar and 3.8, respectively.

Table 5: Summary of water flux and recovery results in the FO

DS initial osmotic pressure (bar)	**DS to FS initial volume ratio**	**Average experimental FO water flux[a] (LMH)**	**Experimental recovery rate @ 2 LMH**
55	2.4	8.1	22 %
80	2	7.7	36 %
80	2.4	7.4	40 %
130	1	6.3	47 %
140	1.4	5.2	49 %
140	2	3.8	55 %

4.3 Predicted productivity of the FO step

The following are chosen outcomes of one-dimensional, system-wide simulations implementing the analytical FO water flux equation. The understanding of the influence of co-current and counter-current configurations is provided by initial exploration. Similar to the FO experiments in the previous chapter, the aforementioned experiments resemble co-current configuration. Although the counter-current configuration yields better recovery rates, it is not practical to apply to a lab scale system. It can be tested using either a pilot or a real scale system. Water flux simulations were limited to a lower flux equal to 2 LMH, as previously mentioned. Expectedly, more uniform fluxes (as a function of recovery rate) and higher recovery rates were obtained via counter-current configurations. Figure 8 presents results obtained with DS to FS flow rate ratio of 2 and NaCl as draw agent.

Remarkably, the predicted achievable recovery rate in counter-current configuration reached a maximum of roughly 79%. Comparing co-current and counter-current configurations, the latter was between 11 % higher for an influent DS osmotic pressure of 60 bar, and 22 % higher for an influent DS osmotic pressure of 160 bar. As depicted in Figure 4b in the previous chapter, at the same membrane area and osmotic pressure, counter-current configuration does not necessarily provide higher recovery rates with respect to co-current configuration. However, introducing a considerably larger membrane area results in higher recovery rate compared to co-current configuration, with a more uniform use of the membrane area. Note that adding membrane area in co-current configuration does not produce benefits, because the associated fluxes would be unfeasibly low in the added portion of the system. In fact,

a counter-current configuration allows better exploitation of a larger amount of membrane area.

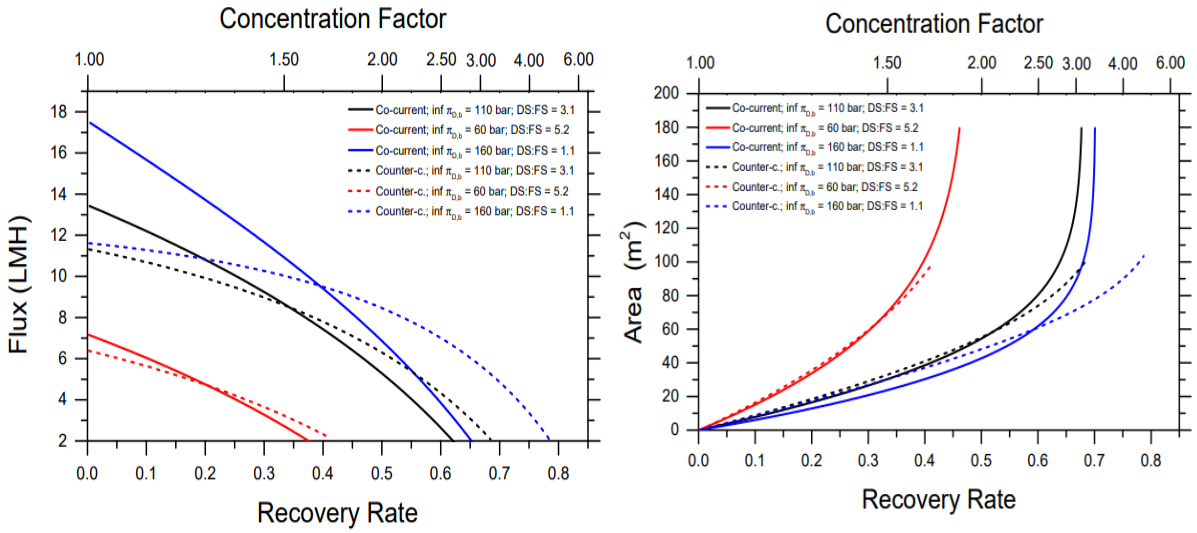

Figure 9: Productivity of an FO system simulated under co-current vs. counter-current configurations.

(a) Water fluxes as a function of recovery rate and concentration factor. (b) Recovery rate as a function of normalized membrane area and concentration factor. Representative results for the case of NaCl as draw agent, a DS to FS influent flow rate ratio of 2, and stopping the simulations at water flux values equal to 2 LMH.

Figure 9 illustrates a comprehensive set of predictions for co-current and counter-current configurations. By varying the influent DS (NaCl) osmotic pressure and the DS to FS volume ratio, a broader comparison between both configurations can be drawn. By interpolation of the obtained achievable recovery rates, the color maps illustrated in Figure 10a-c were generated, which facilitate the prediction of the achievable recovery rate under a wider range of conditions. Observing the data obtained from the simulations, it can be deduced that counter-current configuration is more efficient than co-current. For example, a recovery rate of 70% can be achieved via co-current configuration at DS influent osmotic pressure 160 bar and DS:FS volume ratio of 3, while the same recovery rate can be reached at DS influent osmotic pressure of approximately 130 bar and DS:FS volume ratio of approximately 2.3 via

counter-current configuration. However, it is vital to consider the osmotic pressure of the effluent stream, which must be managed in a safe and environmentally-friendly way. The diluted draw solution may be discharged as a brine (analogously to what currently done for reverse osmosis seawater desalination brine) if its quality meets the legislative standards. For instance, achieving a theoretical 70% recovery via counter-current configuration, a 90-100 bar of DS effluent osmotic pressure will be obtained (as per figure 9d). However, this possibility should be appraised on a case-by-case manner, in accordance with the legislator, and ensuring that the concentrated draw solution does not contain unwanted substances that may pass from the feed to the draw side This must be taken into consideration when planning the target recovery, ideal operating conditions, and effluent management. A practical approach for this challenge would be to utilize the RO brine from seawater desalination plants as the FO influent draw solution. At 55 bar influent osmotic pressure, the recovery rate would be around 30% (as per figure 10c) with DS effluent osmotic pressure of around 45-50 bar (as per figure 10d). Notably, varying DS:FS flow ratio in this circumstance have little effect on recovery and DS effluent osmotic pressure.

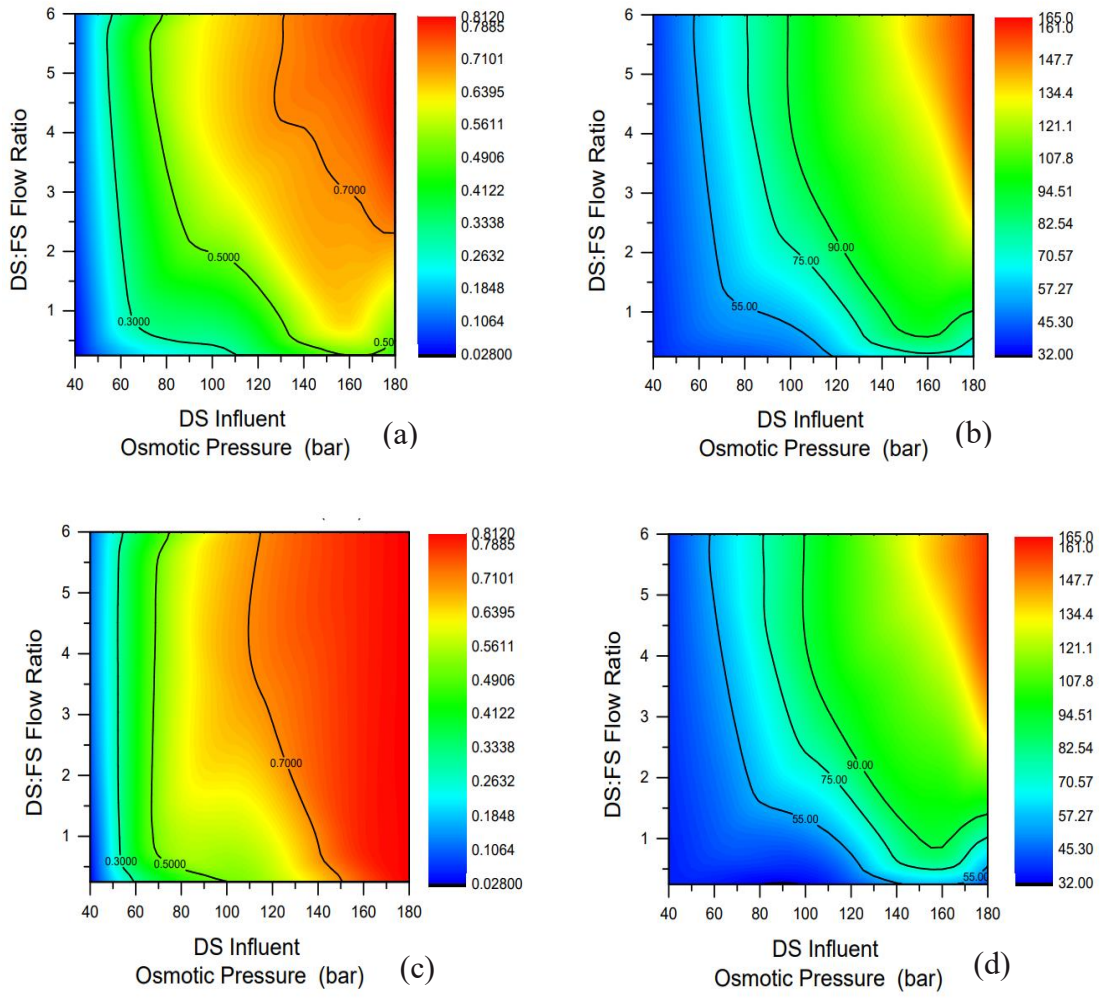

Figure 10: Simulation-based predictions of FO system behavior as s function of DS influent osmotic pressure and DS to FS influent flow rate ratio

(a) achievable recovery rate in the FO step (Co-current mode); (b) Osmotic pressure of effluent draw solution (Co-current mode); (c) achievable recovery rate in the FO step (Counter current mode); (d) Osmotic pressure of effluent draw solution (Counter current mode). Simulations were run with NaCl as draw agent and until a water flux equal to 2 LMH was calculated.

4.4 Quality of the product water

Remarkable retention was observed by the FO membrane during composition analysis of the effluent stream. The average system rejection was 98.9% and 98.3% for TOC and TN respectively, with minimum variance in retention values based on osmotic pressure and FS:DS ratio (Table 6). The highest measured TOC and TN retention (99.4% and 99.1% respectively) was at 80 bar osmotic pressure, and FS:DS

ratio of 2.4, while the lowest TOC and TN retention (97.9% and 96.8% respectively) was observed at 140 bar osmotic pressure and 1.4 FS:DS ratio. In addition, 97.9% is the average system rejection observed for B in the diluted DS.

Table 6: Composition of the diluted draw solutions from the high-recovery FO tests

DS initial osmotic pressure (bar)	DS to FS initial volume ratio	TOC rejection (%)	Na (ppm)	B (ppm)	TN rejection (%)	Effluent osmotic pressure (approx.) (bar)
55	2.4	99.4	19600	0.6	99	45-50
80	2	99.3	26140	0.8	98.9	55-60
80	2.4	99.4	26700	0.6	99.1	60-65
140	1.4	98	47900	1.55	97.1	85-90
140	2	98.9	39300	1	98.3	85-90

5. Conclusion

This study examined the efficiency of using FO for the treatment of amine water, a byproduct of gas sweetening processes. Four draw solutions were initially evaluated to identify the most suitable draw solution to be used for the high recovery experiments. Subsequently, high recovery experiments employing NaCl as the draw solution, while varying draw solution osmotic pressure and draw-to-feed volume ratios, were conducted to further assess the feasibility of the FO process in concentrating rich amine water. FO transport equations were employed for designing simulations. These simulations were then validated using the obtained experimental results. By validating the simulations with experimental results, it allowed the prediction of achievable recovery rate in a broader range of operating conditions. The obtained results suggests that:

1- The highest recovery achieved was 55% using an initial DS osmotic pressure of 140 and a draw-to-feed volume ratio of 2. Notably, high recovery results showed a correlation between initial DS osmotic pressure and larger initial DS to FS volume ratios corresponded to enhanced recovery rates. However, it is important to consider that higher osmotic pressures lead to increased operational costs due the necessity to utilize more robust membranes that can handle high operating pressure. Additionally, complications to the discharge of the effluent draw solution arise due to having a more concentrated draw solution.

2- According to the simulations, the counter-current configuration exhibited superior performance in contrast to the co-current configuration. This suggests that the counter-current configuration offers advantages in terms of system efficiency.

3- Chemical analysis of the concentrated feed and diluted draw showed that the membrane successfully prevented reverse flux. With average total organic carbon (TOC) and total nitrogen (TN) system retention rates of 98.9% and 98.3% respectively, the FO membrane demonstrated robust performance in retaining contaminants and preventing their passage through the membrane.

4- The concentration of rich amine water through FO demonstrates the potential of FO as a possible pretreatment step for managing amine-rich water. This study has shown some effectiveness in concentrating the aqueous stream, which could reduce the volume of effluent requiring further treatment or disposal. This may help industries dealing with amine-rich water, such as gas processing facilities, to enhance the efficiency of their overall wastewater management processes. FO may offer other advantages, such as reduced energy consumption (compared to traditional treatment

methods), which further enhance its appeal as a sustainable solution for handling complex liquid streams like amine rich water.

5- FO Forward osmosis (FO) has several disadvantages that can hinder its widespread adoption. One significant drawback is membrane fouling. Eventually, contaminants can accumulate on the membrane surface, reducing its efficiency. This can be examined in future research to analyze membrane fouling due to amine water concentration. In order to regain efficiency, frequent cleaning or replacement may be required. Additionally, due to prominent levels of contaminants, the disposal of concentrated draw solution can be challenging, as it requires further treatment in advance. These factors can complicate the implementation of FO and may offset some of the potential benefits in certain applications.

Chapter 3: Preliminary Technical Feasibility Study of the Recovery of Used Lubricant Oil (ULO) from Oil & Gas Industry Using Ultrafiltration[3]

1. Introduction

Lubricating oil is a petroleum product that is used for friction reduction in machinery, minimizing wear in moving parts and enhancing the overall output efficiency for moving parts of automotive engines and industrial machinery. Virgin lubricant oil comprises approximately 80-90% base oil and 10-20% chemical additives. These additives are mainly surfactants, such as antioxidants, detergents, viscosity enhancers, as well as rust and wear inhibitors. The wear/oxidation impurities consist of sludge, oxidation products, carbonaceous particles, and ash. These impurities are often composed of a variety of metal elements originating not only from wear, but from the lubricant additives as well [116],[117].

Table 7: Typical composition of ULO

Component	Volume % in ULO
Base oil	65 – 75
Wear / oxidation impurities	10 – 20
Water	5 – 8
Diesel/gasoil	4 – 6
Naphtha/gasoline	2 – 4

[3] This study was performed at VITO, an independent Flemish research organization, from March till June 2023 in the framework of the CUMERI project. CUMERI project aims at customizing membranes, recovering valuable components, and improving energy efficiency in industrial facilities.

Throughout the process of using lubricant oil, the chemistry of the oil changes due to temperature build up, resulting in additives break down, causing corrosion and oxidation. Simultaneously, the level of impurities increases with the change in viscosity, acidity, flash point, and metal content of the oil, leading to inefficient performance of the relevant system, a shortened lifespan of the equipment, and premature failures. Following usage, the quality of oil deteriorates, resulting in the loss of its essential properties and consequently it becomes impotent. [118-121]

The environmental disposal of used lubricating oil (ULO) presents a hazard to soil, water, and air, given its classification as a toxic and non-biodegradable waste [121,122]. Due to the high management costs of ULO, improper enforcement of environmental regulations, and mismanagement of its disposal, waste lubricant oil was commonly dumped into water bodies, causing an increase in chemical oxygen demand (COD), adversely affecting aquatic life [123]. Recently, 80% of the collected ULO undergoes recycling for reuse or regeneration into new products. This change comes in response to the continuous growth in the annual production of used automobile lubricating oil [124]. Numerous approaches are employed to recycle ULO into valuable fuel products or chemical feedstock. In the EU region, ULO is recycled into base oil which is directly re-used for formulation of new lubricants. Some of the current recycling techniques include acid/clay treatment method, solvent extraction, hydrogenation/clay treatment, pyrolysis using microwave heating, and membrane filtration technology such as distillation. [125-128]

The utilization of membrane technology has gained significant traction due to its potential in addressing environmental challenges, enhancing industrial processes, and contributing to sustainable development. With the increasing urgency to mitigate

carbon emissions and control the impact of climate change, the development of advanced membrane technology capable of liquid treatment in the oil and gas industry holds immense significance [128-138]. Within this context, the European Union's Horizon Europe research and innovation program has issued a grant to fund the "CUMERI" project to develop at TRL7 "advanced and customized membrane separation systems in two key industries; the steel sector and the oil and gas industry." CUMERI has managed to attract 15 partners (6 RTOs and 9 companies including 4 SMEs) to reach its research goals and will develop in 36 months three membrane technologies "1- enhanced bio-based and recyclable polymer membranes for CO_2 permeation; 2- stable and selective SiC/SiCN membranes for H_2 recovery in the steel sector; 3- grafted porous ceramic membranes for waste oil purification in the oil and gas sector". Through theoretical and experimental research, the CUMERI project aims to provide solutions into the diverse aspects of membrane technology, incorporating material synthesis, membrane fabrication, characterization techniques, and process optimization. [139],[140]

Several studies in waste oil treatment have incorporated the application of ultrafiltration (UF) membranes for the purification of ULO. Widodo et al. investigated the usage of polypropylene membrane for ultrafiltration of waste engine oils. Operating pressure was varied within the range of 0.4-1.2 bar as well as temperature between 30-60 ^{o}C to examine their effect on membrane flux and rejection. Results showed that higher oil fluxes were attained with increased pressure and temperature, while rejection showed a steady behaviour. Impurities were efficiently removed from the waste oil such as: ash (90–99 %), water (78–82.5 %), zinc (28.9–43.8 %), and calcium (50.1–58.9 %), enhancing the treated oil's viscosity, density, and colour [141]. The same trend

was reported by Nissar et al. who investigated the employment of polyacrylonitrile ultrafiltration membrane to recover the lubricating oil [142]. More than 90% of contaminants and heavy metals were successfully removed by the UF membrane, which improved the properties of the oil in terms of viscosity, colour, and odour. In addition, several membrane materials have been recently proposed to enhance the efficiency of membrane separation for ULO treatment. Cao et al. tested three types of polymer hollow fibre membranes (polyethersulphone (PES), polyvinylidene fluoride (PVDF), polyacrylonitrile) with different pore sizes to recycle ULO. A rejection rate of 99.6% was observed with the UF membrane, surpassing the rejection rates of microfiltration membranes made with PES and PVDF. Both liquidity and flash point of the recovered lubricant oil were highly improved [143]. Although recent studies on ULO recovery have tested different membranes with various pore sizes and materials, this research lacked details for testing grafted ceramic membranes customized for ULO recovery.

This chapter embodies an exploration of grafted porous ceramic membranes for waste oil purification. The effective treatment and purification of waste oils, including used lubricants and industrial oil residues, is crucial for environmental sustainability and resource conservation. Grafted porous ceramic membranes offer an assuring possibility for separating impurities and contaminants from waste oils, enabling the recovery of valuable resources and the minimization of environmental impact. [144]

Building upon the aforementioned work, this research investigates the usage of both native and grafted porous ultra-filtration ceramic membranes for the purification of ULO from the oil and gas industry. Several native and grafted UF membranes were tested for base oil recovery from real life ULO samples. The impact of membrane pore

size, membrane surface modification, and different test conditions on membrane flux and selectivity were examined. The research seeks to contribute to the development of innovative ceramic membrane-based processes for waste oil purification, addressing a critical environmental concern and advancing sustainable practices. In addition, enhancing carbon circularity (reuse of recovered base oil for production of new lubricants) and CO_2 footprint reduction are objectives we strive to achieve.

2. Materials and methods

2.1 Membranes and chemicals

TiO_2 commercial UF ceramic membranes of 25 cm length (monochannel tubes with an outer diameter of 1 cm, and an inner diameter of 0.7 cm) for liquid filtrations were purchased from the company Inopor, Germany. Molecular weight cut-offs (MWCO) shared by the supplier are 8.5, 20, and 100 kDa for the different pore sizes 5, 10, and 30 nm membranes, respectively. The customized membranes were developed using the native ceramic membrane supports and chemically modified them with the right grafting technology. The ceramic support offered chemical robustness and enabled treatment at elevated temperatures ranging from 50 to 150 °C. This temperature range is particularly advantageous for treating viscous ULO feed streams.

In this study, various native membranes featuring different pore sizes (5, 10, and 30 nm) were examined using several ULO streams as feeds under identical conditions. The objective was to clean-up ULO at a decent flux while determining the most suitable pore size for grafting. Different native membranes were grafted using different grafting techniques as shown in table 8. Due to the abundancy of -OH groups on the surface of native TiO_2 NF membranes, the membranes were highly hydrophilic.

Three different chemical modification agents were used for the modification of the surface chemistry of the membranes namely: Grignard reagents (GR), phosphonic acids (PA), and surface-initiated atom transfer radical polymerization (Si-ATRP). Each grafting technique yielded different surface and pore chemistry modifications. Grignard grafting is considered a complex process that requires to be performed in an ether environment free from water. In contrast, phosphonic acids grafting can be easily carried out in water. Additionally, its stability in water has been shown to surpass that of salination. However, a significant limitation of this grafting method is the narrow range of functional groups available for commercial purchase. In comparison, there is a much broader selection of Grignard reagents on the market. A partial replacement of the surface -OH groups of the native membranes occurred when Grignard modification was utilized (as shown in Figure 11), leading to a direct bond of the organic groups to the metal atoms without the involvement of oxygen atom (M-R bond). On the other hand, the phosphonic acid reaction is a condensation reaction that resulted in the formation of one or more oxygen bridging (M-OP-R) bonds [144], [145]. The surface-initiated atom transfer radical polymerization presents a more controlled approach; it is a technique used for the transfer of activated monomer units in order to grow a well-defined polymer chain from the membrane surface. While PA grafting is considered more user-friendly and stable in water, Si-ATRP provides advanced capabilities for designing tailored materials, making each method suitable for various applications based on the desired properties. [146]. In this project, the grafting process was monitored through a permeability test. When the desired permeability was reached, the polymerization was terminated, indicating a decrease in the membrane pore size.

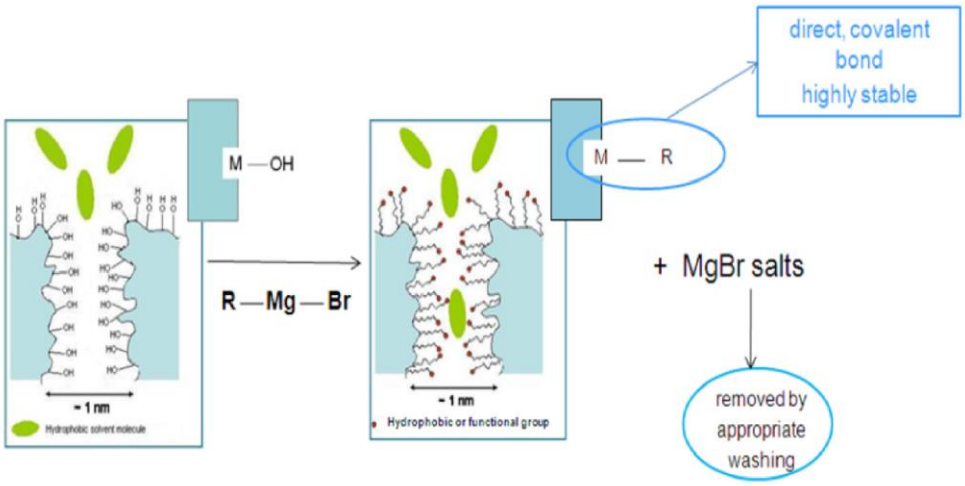

Figure 11: Illustration of ceramic membranes Grignard modification [147]

Table 8: Ceramic UF membranes with different grafting for used lubricant oil purification.

Functional group	Grafting technique	Membrane pore size	Modified membranes code
Methyl	GR	10 nm	10TiO_2-C1
Pentyl	GR	10 nm	10TiO_2-C5
Octyl	GR	10 nm	10TiO_2-C8
Dodecyl	GR	10 nm	10TiO_2-C12
Octadecyl	GR	10 nm	10TiO_2-C18
Phenyl	GR	10 nm	10TiO_2-Ph
Polystyrene	Si-ATRP	10 nm	10TiO_2-PS
Phenyl	PA	10 nm	10TiO_2-PPA
Octyl	GR	5 nm	5TiO_2-C8

2.2 Feed Solutions Characteristics.

Several lubricant oils, sourced from the company OSILUB, were tested as feed in the UF experiments. The ULO obtained from OSILUB is a mixture that is sourced from various trucks, with approximately 90% obtained from cars and 10% from industrial applications. As shown in Figure 12, different pre-treatments were performed

on the ULO prior to the UF membrane treatment; starting from the cleanest lubricant oil to the more complex:

1. Commercial formulated lubricant oil, code 15W-40
2. Feed streams received from OSILUB:
    - OSIL150 base oil product
    - ULO without neutralization (OSILUB 2)
    - ULO after 1st distillation as a pre-treatment (OSILUB 4)
    - ULO after 2nd distillation as a pre-treatment (OSILUB 5)

The ULO tested in this study were categorized depending on the level of pre-treatment. OSILUB 2 is the ULO without neutralization or pre-treatment, OSILUB 4 is the ULO after applying the 1st distillation to remove water and naphtha, and OSILUB 5 is the ULO after applying the 2nd distillation to remove diesel. In addition, neutralization of ULO by adding sodium hydroxide before pre-treatment was an essential step to avoid the effect of acidic organic compounds forming during lubricant oil use in the distillation columns. The various pre-treatment steps following the neutralization step showed an effect on the viscosity of the UF feed due to removal of high boilers (additives) in distillation columns, for instance the removal of Zn and Ca as shown in table 10, potentially causing variations in the obtained flux during UF.

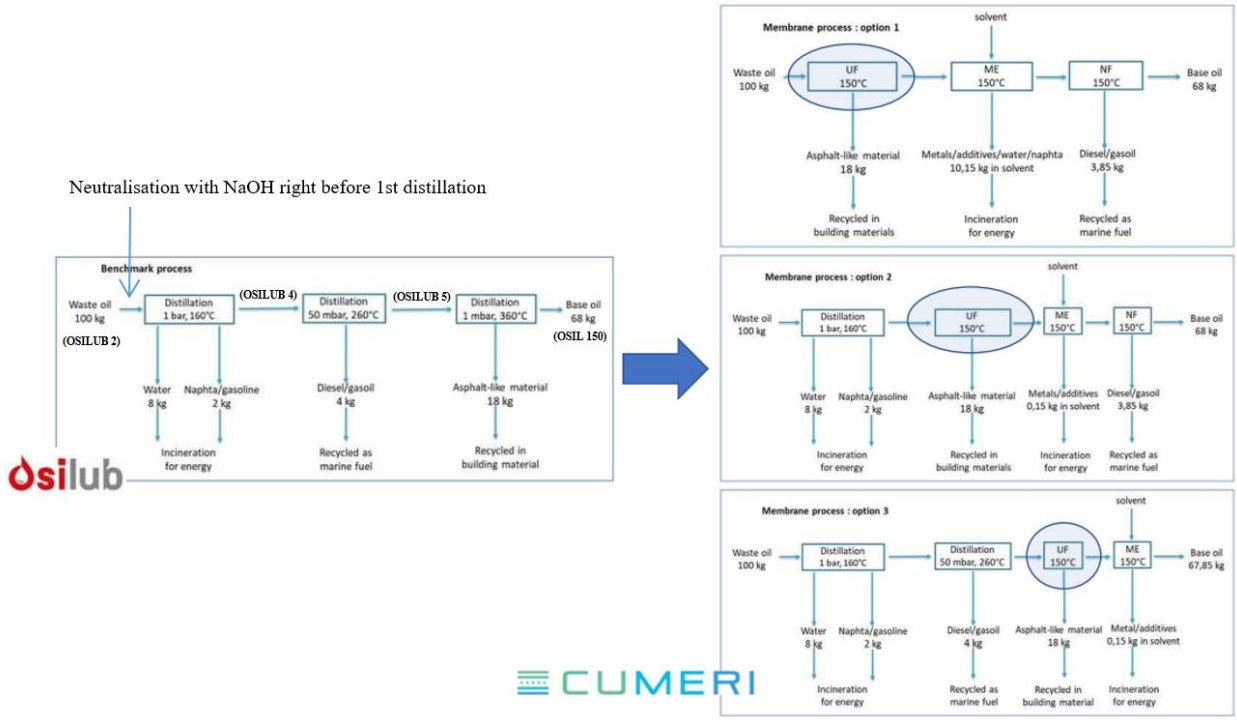

Figure 12: Different feeds used in the UF. All membranes were tested using the clean commercial lubricant oil, while industrial ULO process streams from Osilub were only tested with a selected set of membranes.

2.3 Properties of different ULOs in this study

Tables 9 and 10 below presents the properties of ULO samples described in section 2.2.

Table 9: Characteristics of the ULOs

Feed streams	Water (ppm)	Visc. at 40°C (cSt)	Visc. at 100°C (cSt)	TAN (mg KOH/g)	Oxidation (Abs/0.1 mm)	Nitration (Abs/0.1 mm)	Diesel %	Naphtha %
Clean LO	158	95.5	13.8	1.91	5.9	4.1	-	-
OSILUB 2	63000	53	8.7	1.96	29	24.4	5.8 - 7	1 - 6.8
OSILUB 4	870	56.1	9.9	0.83	20.9	11.3	4.5 - 5.5	0.5
OSILUB 5	119	58.4	9.9	0.59	19.9	8.5	-	-
OSIL 150	20	28.4	5.3	0.07	7.6	2.5	-	-

Table 10: Metal content of different ULOs (Additives, wear, and contaminations content)

	Additive (ppm)						Wear (ppm)							Contamination (ppm)		
Feed	**Ba**	**Ca**	**Mg**	**P**	**S**	**Zn**	**Mo**	**Al**	**Cu**	**Cr**	**Fe**	**Pb**	**Sn**	**Na**	**B**	**Si**
Clean LO	<0.25	2183.3	561.6	935	5500	1010	92	1.7	0.4	<0.25	0.94	0.8	<1	2.6	<1	15
OSILUB 2	3	1260	98	580	3400	630	43	12	18	<5	83	<5	8	76	168	60
OSILUB 4	3	1360	121	672	3500	624	49	13	18	<5	92	11	9	1098	148	63
OSILUB 5	3	1530	139	744	2900	699	54	19	18	<5	106	12	8	1400	133	63
OSIL 150	<1	<5	<5	12	1300	<5	<5	<5	<5	<5	<5	<5	<1	<5	20	17

2.4 Membrane filtration setup

The UF experiments were conducted with a crossflow lab scale system. The system comprised of a feed vessel that accommodated up to 1 L of liquid, a high-pressure circulation pump for cross-flow, bit nitrogen gas for pressurization, cylindrical membrane housing cell, temperature control, and data acquisition system (see Figure 13). The entire setup was covered with a heat insulation system to minimize heat loss during the experiment. During the experiment, the retentate stream was recirculated back to the feed reservoir, while the permeate stream was continuously collected in an external vessel.

Figure 13: Crossflow lab scale setup system

2.5 UF tests and varying operational parameters tests.

The UF tests were carried out as follows: 1 liter of lubricant oil was introduced into the feed tank and circulated at a velocity of 2 m/s. Simultaneously, the oil was heated to achieve a temperature of 110 °C. Once temperature was stabilized at 110°C, a 100 mL feed sample was collected. Then, the pressure was elevated to 10 bar, and a 100 ml permeate sample was collected, aiming for 11% recovery in all tests. Throughout the process, the flux was measured, and operational conditions were continuously monitored. Finally, a 100 mL retentate sample was collected. All samples were analyzed by external service lab “Alpha Maintenance Systems”.

Varying operational parameters including feed pressure, temperature, and cross flow velocity to assess their impact on membrane performance (in terms of oil flux and impurities rejection) were also examined. Following the same previous procedure, the feed pressure was varied in three consecutive steps (5, 10, 15 bar). At each step, 30 mL sample of permeate was collected. Following the same methodology, temperature's influence was examined by varying it in three successive steps (80, 100, and 110 °C). Additionally, the impact of crossflow velocity was examined by varying it in four steps (2, 4, 1, then 2 m/s) while maintaining other operational parameters constant. The systematic and sequential adjustments in the operational parameters ensured a thorough exploration of their individual impacts on the separation process.

3. Results of Clean Lubricant Oil

3.1 Effect of membrane grafting and pore size

- **Flux:**

Different membranes with varying grafting were examined at the same operating conditions of 10 bar and 110 °C in order to evaluate their performance in filtering clean lubricant oil as shown in table 11. The results showed that despite employing diverse surface modifications and grafting techniques, the resulting fluxes demonstrated minimal variance, ranging from 4.3 to 5.3 Kg $h^{-1}m^{-2}$, except for the 5 nm native membrane that had a flux of 7.5 Kg $h^{-1}m^{-2}$. This suggested that grafting had negligible influence on membrane performance and that other factors, beyond grafting, may play a more essential role in determining flux behavior. These factors are bulk viscosity, cake layer formation, and different operating parameters (temperature, pressure, and cross-flow), which have more impact on these phenomena than membrane chemistry. The highest flux value was achieved by the 10TiO_2-C5 membrane (5.6 Kg $h^{-1}m^{-2}$). In addition, membranes with different pore sizes were also evaluated. Unexpectedly, the variation in pore size also had negligible influence on the obtained fluxes. These findings challenged conventional assumptions regarding the correlation between pore size and flux in membrane processes while treating lubricant oil [130]. These phenomena might be due to the formation of a cake layer on the surface of the membranes as a result of retaining heavy additives. This cake layer acts as a secondary membrane, impacting not only flux but also impurity retention.

In case of the 10 nm native membrane, the obtained flux was approximately half that of the 5 nm native membrane. The reason for this difference in flux was the

10 nm membrane pore size being close to the size of impurities in the feed lubricant oil (in the range of 10 nm). Consequently, the additives clog the membrane pores under pressure, and thus reducing the flux. On the other hand, for the native 5 nm membrane, the impurities remain on the surface of the membrane and does not clog the membrane pores, therefore maintaining a higher flux.

Following the 5 nm native membrane, the three membranes, namely $10TiO_2$-C1, $10TiO_2$-C5, and $10TiO_2$-C8 had the highest flux among grafted membranes. These membranes contained hydrophobic functional groups. However, the difference lied in the chain length of these functional groups and their respective coverage on the membrane surface due to the steric and kinetic effects during Grignard grafting. 10TiO2-C1 had the shortest chain length compared to the other two, resulting in the highest coverage. On the other hand, $10TiO_2$-C8 exhibited lower coverage due to the longer chain, causing steric hinderance to the remaining -OH groups on the membrane surface. $10TiO_2$-C5 demonstrated the optimum performance, as its medium chain length resulted in medium coverage, therefore it exhibited the highest flux.

Table 11: Membranes' performances using clean lubricant oil as feed

Membrane	Flux (Kg $h^{-1}m^{-2}$)
10 nm	4.7
10 nm re-used	4.3
10TiO_2-C1	4.9
10TiO_2-C5	5.6
10TiO_2-C8	5.3
10TiO_2-C12	4.5
10TiO_2-C18	4.5
10TiO_2-Ph	4.4
10TiO_2-PS	4.5
10TiO_2-PPA	4.5
5 nm	7.8
5TiO_2-C8	4.5
30 nm	4.6

- **Impurities Rejection and Quality of the Treated Oil:**

Based on the analysis of the UF-treated clean lubricant oil, all tested membranes managed to effectively reduce water, viscosity, acidity, oxidation, and nitration. The data presented in tables 12 and 13 outline the performance of the 10 nm membrane in treating clean commercial lubricant oil. Upon filtration, viscosity of the clean oil was reduced by 61% and 57% at 40 ºC and 100 ºC, respectively. In addition, 63% reduction in the Total Acid Number (TAN) was observed, while oxidation and nitration levels were reduced by 48% and 37%, respectively. Additionally, metals such as Ca, Mg, and Mo were completely removed, achieving up to 100% elimination by the UF

membranes. However, the removal efficiency differed for other metals, with P, Zn, and Fe exhibiting a retention rate of 40%. S and Cu showed a lower removal efficiency, with only 20% rejection rate. Membrane grafting and/or pore size had minimal influence on retentions except for water retention, which showed a correlation with the membrane pore size. Varying retention rates were obtained for water across different membrane pore sizes, with 5 nm membrane retaining 73%, 10 nm membrane retaining 67%, and 30 nm membrane retaining 46%.

3.2 Filtration performances of the native 10 nm membrane for clean lubricant oil

Table 12: Characteristics of the feed, retentate, and permeate of clean lubricant oil after UF

Clean LO	Water (ppm)	Visc. at 40°C (cSt)	Visc. at 100°C (cSt)	TAN (mg KOH/g)	Oxidation (Abs/0.1 mm)	Nitration (Abs/0.1 mm)
Feed	158	95.5	13.8	1.91	5.9	4.1
Retentate	150	100	15	3.00	6.3	4.3
Permeate	50	39	6.5	1.12	3.3	2.7
Retention	67%	61%	57%	63%	48%	37%

Table 13: metal content of the treated clean lubricant oil using 10 nm membrane (Additives, wear, and contaminations content)

	Additive (ppm)						Wear (ppm)							Contamination (ppm)			
	Ba	**Ca**	**Mg**	**P**	**S**	**Zn**	**Mo**	**Al**	**Cu**	**Cr**	**Fe**	**Pb**	**Sn**	**Na**	**B**	**Si**	**Sum**
Feed	<0.25	2183.33	561.67	935	5500	1010	92	1.07	0.4	<0.25	0.94	0.8	<1	2.6	<1	15	10302.81
Perm 10nm	<0.25	2.00	1.00	650	4900	660	1.00	<0.5	0.30	<0.25	0.60	0.80	1.00	0.80	<1	3	6220.50
Average. Retention		100%	100%	36%	20%	40%	99%		25%		36%	0				70%	40%

The permeate had visibly brighter colour when compared to the feed and retentate as shown in figure 14. This might be due to the reduction of additives present in the permeate after UF.

Figure 14: Clean lubricant oil before and after UF treatment using 10 nm native membrane.

3.3 Effect of Temperature for Native 10 nm

As shown in Table 14, increasing the temperature of the feed during the UF experiment enhanced the obtained fluxes. As the temperature increased to 100°C, the flux rose notably from 3.85 to 4.05/4.50 Kg $h^{-1}m^{-2}$, indicating enhanced oil flow. Notably, two flux values measured suggested a potential fluctuation in flow behaviour at this temperature. Moreover, the kinematic viscosity decreased to 13.8 cSt, and density decreased to 767 kg/m³. Further increase in the temperature to 110 °C resulted in a higher flux (4.66 Kg $h^{-1}m^{-2}$) and even lower kinematic viscosity (10.4 cSt). This indicated a substantial reduction in oil viscosity with increasing temperature. Consequently, this enhanced the mass transfer of oil through the membrane, resulting in higher fluxes [141,148,149]. As shown in Figure 15, flux is dependent on dynamic viscosity indicating that flux increases when dynamic viscosity decreases. In addition, density reduction suggests that heavy additives existing in the oil are reduced.

Table 14: 10 nm membrane performance at various temperature and constant pressure (10 bar)

T (°C)	Flux (Kg $h^{-1}m^{-2}$)	Kin Visc. (cSt)	Density (	~1/(dyn. visc.)
40	--	95.5	804	0.42
80	3.85	21.9	780	1.78
100	4.50 / 4.05	13.8	767	2.78
110	4.66	10.4	760	3.65

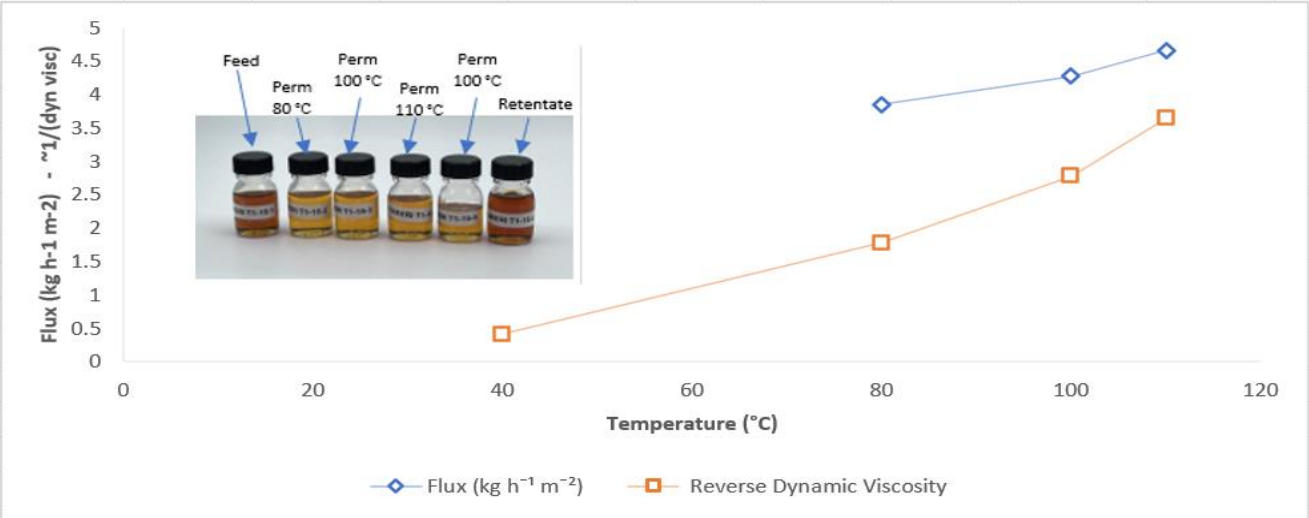

Figure 15: Effect of temperature on flux & reverse dynamic viscosity of clean lubricant oil during UF.

3.4 Effect of Pressure for Native 10 nm

Table 15 show the relationship between pressure and flux during the testing of clean lubricant oil. As pressure increased from 5 to 10 bar, there was a slight increase in flux from 4.85 to 4.87 Kg $h^{-1}m^{-2}$ due to the increase of solute concentration in contact with the membrane surface. This resulted in higher flux. However, as the pressure continued to rise to 15 bar, the flux decreased to 4.76 Kg $h^{-1}m^{-2}$ and kept declining to 4.68 Kg $h^{-1}m^{-2}$ at 10 bar. Finally, the lowest flux achieved was 4.57 Kg $h^{-1}m^{-2}$ at the initial pressure of 5 bar. The slight fluctuations in flux with pressure

implied a non-linear relationship with pressure. This might be due to the formation of a cake layer acting as a secondary membrane due to additive retention. The cake exhibits a high level of compressibility, as indicated by the nearly constant flux. However, when the pressure was reversed, slightly lower fluxes were observed. This reduction in flux can be attributed to factors such as pore clogging and the consolidation of a fouling layer.

Table 15: 10 nm membrane performance at various pressure and constant temperature (110°C)

Pressure (bar)	Flux (Kg $h^{-1}m^{-2}$)
5	4.85
10	4.87
15	4.76
10	4.68
5	4.57

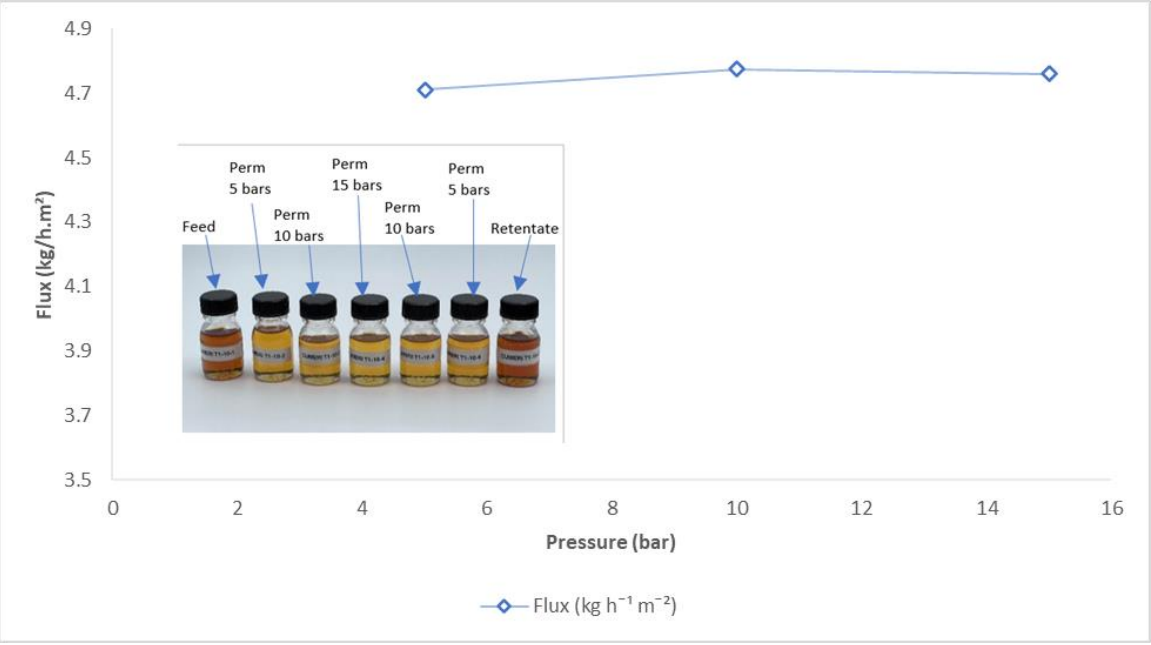

Figure 16: Effect of pressure on flux of clean lubricant oil during UF.

4. Results of base oil OSIL150

Filtration performances of the 5, 10, and 30 nm membrane for OSIL150

OSIL150 was tested under the same conditions as the commercial lubricant oil, with a temperature of 110 °C, pressure of 10 bar, and crossflow velocity maintained at 2 m/s, using the same native TiO_2 UF membranes with varying the pore size (5, 10, and 30 nm). Table 16 reveals that OSIL150 yielded higher fluxes compared to the commercial lubricant oil when tested with the same membranes due to the absence of additives in OSIL150, resulting in lower viscosity, thereby no formation of a cake layer. As expected, the 30 nm membrane exhibited the highest flux of 300 Kg $h^{-1}m^{-2}$, followed by the 10 nm membrane (70 Kg $h^{-1}m^{-2}$), and finally the 5 nm membrane (20 Kg $h^{-1}m^{-2}$). The obtained fluxes displayed a high decline rate over time to collect 100 mL permeate.

The chemical analysis of the feed, permeate, and retentate samples indicated that the quality of the permeate did not change from the feed, suggesting that retention remains unaffected by membrane pore size, as shown in table 17. This means that the remaining contaminants in the base oil OSIL150 are too small in size to be retained by UF. Only water retention, mostly free water, showed a dependency on the membrane pore size, a lower pore size correlated with higher water retention.

Table 16: Fluxes and water retention of the 5, 10, and 30 nm membrane for OSIL150

Membrane pore size (nm)	**Flux (Kg $h^{-1}m^{-2}$)**	**Water Retention**
5	20 declined to 4,8	32%
10	70 declined to 11	15%
30	300 declined to 240	-15%

Table 17: Characteristics of the feed, retentate, and permeate of OSIL150 using 10 nm UF membrane.

OSIL 150	Water (ppm)	Visc. at 40°C (cSt)	Visc. at 100°C (cSt)	TAN (mg KOH/g)	P (ppm)	Si (pmm)	B (ppm)	S (ppm)
Feed	38	28	5.5	0.14	12	17	21	1200
Retentate	80	28	5.6	0.14	10	17	20	1250
Permeate	68	28	5.6	0.14	10	17	20	1250
Retention	0.15	0.00	0.00	0.00	0.00	0.00	0.00	0.00

5. Results of ULO feed streams

Filtration performances of the 10 nm membrane for different ULO feed streams

Three ULOs, namely OSILUB 2, OSILUB 4, and OSILUB 5, were assessed using native 10 nm membranes under the same conditions previously used with both the commercial lubricant oil and OSIL150. The flux results obtained for OSILUB 2, OSILUB 4, and OSILUB 5 are 9.08 Kg $h^{-1}m^{-2}$, 8.81 Kg $h^{-1}m^{-2}$, and 9.76 Kg $h^{-1}m^{-2}$, respectively. Throughout the experiments, fluxes remained stable without fluctuations due to cake layer formation, similar to clean lubricant oil. It was observed that the fluxes obtained from testing different ULO feed streams were nearly double the fluxes acquired when testing the clean commercial lubricant oil using the same 10 nm membrane. This can possibly be due to degradation of additives during the use of lubricant oil, dilution caused by water and fuels entering in ULO during use, and storage.

The qualities of the obtained permeates were also analyzed for impurities removal as shown on table 19. Comparing the obtained results with the analysis of each feed stream before applying UF (table 10) shows a strong removal of the water content,

mostly emulsified water, in all the obtained permeates, with average retention reaching approximately 88%. Significant reductions are also observed in oils viscosity, acidity, oxidation/nitration components, and metals. Moreover, when coupled with pre-treatments, further retentions are achieved, particularly in the removal of water, acidity, and metals. Several metal retentions approach 100%, including calcium, magnesium, boron, sodium, iron, and molybdenum. On the other hand, other metals such as: phosphorus, sulfur, zinc, silicon, and copper, showed less rejection rates. This is aligning with the rejections observed in clean lube oil treatment.

Table 18: Characteristics of ULO feed streams after UF using 10 nm membrane.

	Water ppm	Water ppm retention	Visc. at 40°C (cSt)	Visc. at 40°C retention	Visc at 100°C (cSt)	Visc. at 100°C retention	TAN (mg KOH/g)	TAN retention	Oxid. (Abs/0.1 mm)	Oxid. retention	Nitr. (Abs/0.1 mm)	Nitr. retention	Diesel %	Diesel retention	Naphtha %
OSILUB 2	4400	93.0%	24.6	53.6%	6.1	30.0%	0.81	58.7%	14.8	49.0%	4.6	81.1%	6	0	0.5
OSILUB 4	168	80.7%	24.8	55.8%	5.2	47.5%	0.34	59.0%	13.4	35.9%	3.6	68.1%	4.8	0	-
OSILUB 5	12	89.9%	30	48.6%	5.8	41.4%	0.29	50.8%	15.9	20.1%	3.4	60.0%	-	-	-
Average retention		87.9%		52.7%		39.6%		56.2%		35.0%		69.7%		0	

Table 19: Metal content of the treated ULO feed streams using 10 nm membrane (Additives, wear, and contaminations content)

	Additive (ppm)						Wear (ppm)							Contamination (ppm)		
	Ba	**Ca**	**Mg**	**P**	**S**	**Zn**	**Mo**	**Al**	**Cu**	**Cr**	**Fe**	**Pb**	**Sn**	**Na**	**B**	**Si**
OSILUB 2	<1	69	8	343	2900	217	<5	<5	18	<5	7	6	1	2	12	39
OSILUB 4	<1	34	6	240	2600	84	<5	<5	8	<5	2	<5	<1	48	16	28
OSILUB 5	<1	<1	<5	24	1700	<5	<5	<5	<5	<5	5	<5	<1	9	16	31

Table 20: Metal rejection of the treated ULO feed streams using 10 nm membrane

	Additive						Wear							Contamination		
	Ba	**Ca**	**Mg**	**P**	**S**	**Zn**	**Mo**	**Al**	**Cu**	**Cr**	**Fe**	**Pb**	**Sn**	**Na**	**B**	**Si**
OSILUB 2	-	96%	94%	56%	28%	73%	>92%	>71%	0.00	-	94%	0.00	89%	>96%	95%	>96%
OSILUB 4	-	98%	96%	68%	30%	88%	>91%	>71%	56%	-	95%	>44%	89%	96%	91%	96%
OSILUB 5	-	100%	>97%	97%	47%	99%	>93%	>71%	79%	-	96%	0.00	>91%	96%	91%	96%

6. Effect of Crossflow Velocity

The impact of cross flow velocity on the membrane flux was investigated using a native 10 nm membrane with OSILUB 2 as the feed. The experiment involved varying the crossflow velocities at four different values: 2, 4, 1, and 2 m/s. At a cross flow velocity of 2 m/s, the flux measured 7.46 Kg $h^{-1}m^{-2}$; doubling the velocity to 4 m/s caused an increase in flux to 9.57 Kg $h^{-1}m^{-2}$. On the other hand, reducing the velocity to 1 m/s resulted in a decrease in flux to 5.62 Kg $h^{-1}m^{-2}$. Finally, reverting to a cross flow velocity of 2 m/s yielded an increase in flux to 10.52 Kg $h^{-1}m^{-2}$. The results showed a proportional relationship between cross flow velocity and fluxes obtained as higher velocities enhance mass transfer and subsequently increase the flux.

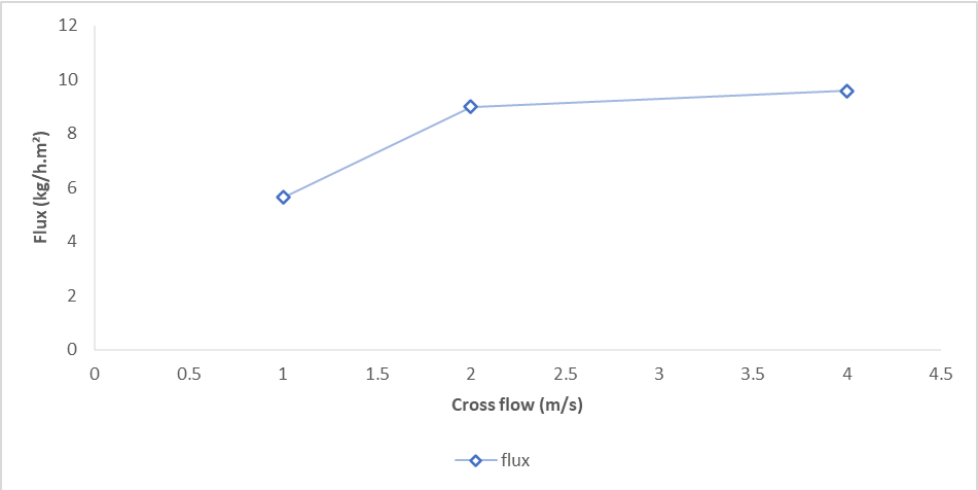

Figure 17: Effect of crossflow velocity on flux of OSILUB2 during UF

7. Conclusion

Ultrafiltration offers the opportunity to reuse waste lubricant oil by removing impurities, which ultimately contributes to decreasing waste disposal to the environment. As depicted above, TiO_2 membrane with different pore sizes and various grafting functionalizations were tested to choose the optimal membrane with the highest fluxes and impurities rejection. The 5 nm native membrane showed the highest flux of 7.8 Kg/h.m^2, followed by the 10TiO_2-C5 membrane with a flux of 5.8 Kg/h.m^2 using clean commercial lubricant oil as feed. Using native 10 nm UF membrane effectively removed impurities when tested with clean lubricant oil. For the latter, water content was reduced by 67%, viscosity (at 40 ^oC) by 61%, TAN by 63%, oxidation by 48%, and nitration by 37%. A visible improvement of the permeate colour was also observed when compared with the colour of the feed solution. In addition, membrane performance as a function of temperature (40-110 °C), operating pressure (5-15 bar), and cross flow velocity (1-4 m/s) was also investigated. Results showed that increasing the temperature induced an increase in the flux and a decrease in the kinematic viscosity and density of the clean lubricant oil. Additionally, increasing pressure raised the flux to a certain point, then flux exhibited a reduction with pressure increase due to membrane pore clogging. Lastly, increasing the crossflow velocity increased the obtained fluxes.

Other feed streams were also tested using 5, 10, and 30 nm native membranes. when OSIL150 was used as feed with the 30 nm membrane, it exhibited the highest flux of 300 kg/hm², followed by the 10 nm membrane with a flux of 70 kg/hm², and finally the 5 nm membrane with a flux of 20 kg/hm². However, quality of the permeate remained unchanged regardless of the membrane pore size except for water retention.

Other feed streams, OSILUB 2, OSILUB 4, and OSILUB 5 had fluxes of 9.08 Kg $h^{-1}m^{-2}$, 8.81 Kg $h^{-1}m^{-2}$, and 9.76 Kg $h^{-1}m^{-2}$, respectively, when tested with 10 nm native membranes. In addition, 88% average water retention was obtained with a major decrease the viscosity, acidity, oxidation/nitration components, and metals content.

In future research, the impact of pore size variation on ULO with different pre-treatments can still be further experimented. Additionally, assessing the feasibility of sulfur removal and the elimination of diesel constituents may be explored. Further study can also be conducted on membrane cake formation due to lower crossflow velocity of the ULO by calculating Reynold's number to strengthen its interpretation. Direction of future research should aim at enhancing our understanding of membrane-based oil treatment processes and potentially contribute to the development of more efficient and sustainable oil purification methods.

Conclusions

Improper liquid waste treatment and disposal from oil & gas industry can have both environmental and economic detrimental effects. This study focused on the use of membrane technology for the treatment of produced water, amine water, and used lubricant oils. Synthetic produced water and amine water were experimented using forward osmosis. Ultrafiltration was the method of choice for experimenting on the treatment and recovery of used lubricant oils. Overall, these methods provided viable treatment solutions to waste liquids from the oil & gas industry, with each method having its own merits. It is crucial, however, to also highlight the challenges for each method used, and the viable solutions and/or further studies that can overcome those challenges.

The process of forward osmosis followed by nanofiltration for the treatment of synthetic produced water and the regeneration of the draw solution is only partly technically viable. $MgCl_2$ was tested as draw agent at various osmotic pressures and draw-to-feed ratios in order to determine the ideal parameters to achieve the highest recovery, with modelling to validate the data and to explore different conditions. The combination of FO followed by NF achieved up to 73% water recovery for the specific feed solution investigated, but with important loss of draw agent, which suggests the need to replenish the draw agent continuously. Also, the results suggest the potential need of using reverse osmosis membranes instead of NF membranes for the draw agent recovery. Further improvements to this study may include the use of real produced water samples and economic calculations to gain insight into the economic viability of the most promising configurations.

Concentration of amine water (a byproduct of gas sweetening processes) was experimented using forward osmosis. The most suitable draw solution (NaCl) was used for high recovery experiments. Varying osmotic pressure and draw-to-feed volume ratios, experimental and simulated results were combined to estimate achievable recovery rate under a broad range of operating conditions, once again supported by modelling by deploying the analytical FO equations. As expected, high osmotic pressure combined with larger initial DS-to-FS volume ratio yielded higher recovery rates, with the highest recovery achieved being 55%. Counter-current configuration proved as superior to co-current configuration in terms of system efficiency. Nevertheless, it is important to note that higher osmotic pressures would ultimately result in increased operational costs and possible complications in managing or discharging the effluent draw solution. The membrane mostly succeeded in preventing reverse flux, with high retention rate of TOC and TN observed. Overall, FO demonstrated medium to high potential in dewatering amine water; however, challenges, such as membrane fouling (which requires constant cleaning and/or membrane changeout depending on operating conditions) still stand. Overall, the practical application of this method would require careful study of the system objectives, costs, and legal limitations.

Finally, several lab scale tests were performed for the recovery of ULO using UF membranes with different pore sizes (10 nm, 30 nm, and 5 nm). The obtained results showed that suitable purity, yield, and viscosity retention were achieved using the 10 nm ceramic UF membranes. This was further examined using not only native ceramic membranes, but also grafted ceramic membranes. In addition, different feed oils were tested; clean lube oil, base oil, ULO after a first pre-treatment (using a distillation

column), ULO after a second pre-treatment (using a second distillation column), and crude ULO. Tests performed using clean lube oil as a feed showed a stable flux with time, with no observable influence of membrane pore size or grafting chemistry. In addition, up to 100% removal of several metals, such as Ca, Mg, and Mo was observed, while other elements, such as P, Zn, and Fe, were partially removed. High declining fluxes were obtained when testing base oil as the feed stream with native membranes. Moreover, fluxes were pore size dependent. Finally, testing different ULO with different pre-treatment as feed streams using native 10 nm membrane resulted in a stable flux that was independent from the feed type. High removal of metals, such as Ca, Mg, and Mo was observed, while other elements, such as P, S, Zn, Si, were retained at a lower rate by the membrane, similar to the results obtained for the clean lube oil.

Based on the conducted literature review and experimental results of this study, membrane technology demonstrates technical promise in treatment of different liquid streams and from the oil & gas industry. While the experimental results highlight the positive outcomes, it is vital to consider economic and legal limitations in managing the effluent solutions that may require further treatment before safely discharging into the environment.

References

1. Munirasu, S., Haija, M. A., & Banat, F. (2016). Use of membrane technology for oil field and refinery produced water treatment—A review. *Process safety and environmental protection*, *100*, 183-202.

2. Fakhru'l-Razi, A., Pendashteh, A., Abdullah, L. C., Biak, D. R. A., Madaeni, S. S., & Abidin, Z. Z. (2009). Review of technologies for oil and gas produced water treatment. *Journal of hazardous materials*, *170*(2-3), 530-551.

3. R. Wagner, Fundamentals Gas Sweetening, Laurance Reid Gas Conditioning Conference, February 26 - March 01, 2006, Norman, Oklahoma

4. Arthur, J. D., Langhus, B. G., & Patel, C. (2005). Technical summary of oil & gas produced water treatment technologies. *All Consulting, LLC, Tulsa, OK*.

5. SRS. Salim, Treatment of amine wastes generated in industrial processes. IOP Conference Series: Materials Science and Engineering. Vol. 1092. No. 1. IOP Publishing, 2021

6. Yang, J., Sun, J., Wang, R., & Qu, Y. (2023). Treatment of drilling fluid waste during oil and gas drilling: a review. *Environmental science and pollution research*, *30*(8), 19662-19682.

7. MS. Islam et al., Degradation studies of amines and alkanolamines during sour gas treatment process. International Journal of Physical Sciences 6.25 (2011) 5877-5890

8. Khammo, M., Obedkov, A., Aljarwan, R., Alhebshi, M., Alnuaimi, H., Almri, M., & Hassan, A. (2024, May). Advanced Produced Water Management in the Oil and Gas Industry: A Comprehensive Examination of Cutting-Edge Treatment Technologies. In *SPE Gas & Oil Technology Showcase and Conference* (p. D021S016R002). SPE.

9. C.V. Simmons, Reclaiming Used Amine and Glycol Solutions, 04 March - 06 March 2006, Norman, Oklahoma.

10. Hamad, A., Al-Zubaidy, E., & Fayed, M. E. (2005). Used lubricating oil recycling using hydrocarbon solvents. *Journal of environmental management*, *74*(2), 153-159.

11. Koroteev, D.; Tekic, Z. Artificial Intelligence in Oil and Gas Upstream: Trends, Challenges, and Scenarios for the Future. *Energy AI* **2021**, *3*, 100041. https://doi.org/10.1016/j.egyai.2020.100041.

12. Madsen, P.T.; Hansen, D.S.; Sperling, K.; Houeland, C.; Jenkins, K.E.H. Abandoning Fossil Fuel Production: What Can Be Learned from the Danish Phase-out of Oil and Gas? *Energy Res. Soc. Sci.* **2023**, *103*, 103211. https://doi.org/10.1016/j.erss.2023.103211.

13. Scanlon, B.R.; Ikonnikova, S.; Yang, Q.; Reedy, R.C. Will Water Issues Constrain Oil and Gas Production in the United States? *Environ. Sci. Technol.* **2020**, *54*, 3510–3519. https://doi.org/10.1021/acs.est.9b06390.

14. Jiménez, S.; Micó, M.M.; Arnaldos, M.; Medina, F.; Contreras, S. State of the Art of Produced Water Treatment. *Chemosphere* **2018**, *192*, 186–208. https://doi.org/10.1016/j.chemosphere.2017.10.139.

15. Rahm, B.G.; Bates, J.T.; Bertoia, L.R.; Galford, A.E.; Yoxtheimer, D.A.; Riha, S.J. Wastewater Management and Marcellus Shale Gas Development: Trends, Drivers, and Planning Implications. *J. Environ. Manag.* **2013**, *120*, 105–113. https://doi.org/10.1016/j.jenvman.2013.02.029.

16. Al-Ghouti, M.A.; Al-Kaabi, M.A.; Ashfaq, M.Y.; Da'na, D.A. Produced Water Characteristics, Treatment and Reuse: A Review. *J. Water Process Eng.* **2019**, *28*, 222–239. https://doi.org/10.1016/j.jwpe.2019.02.001.

17. Kondash, A.J.; Albright, E.; Vengosh, A. Quantity of Flowback and Produced Waters from Unconventional Oil and Gas Exploration. *Sci. Total Environ.* **2017**, *574*, 314–321. https://doi.org/10.1016/j.scitotenv.2016.09.069.

18. Alzahrani, S.; Mohammad, A.W. Challenges and Trends in Membrane Technology Implementation for Produced Water Treatment: A Review. *J. Water Process Eng.* **2014**, *4*, 107–133. https://doi.org/10.1016/j.jwpe.2014.09.007.

19. Fakhru'l-Razi, A.; Pendashteh, A.; Abdullah, L.C.; Biak, D.R.A.; Madaeni, S.S.; Abidin, Z.Z. Review of Technologies for Oil and Gas Produced Water Treatment. *J. Hazard. Mater.* **2009**, *170*, 530–551. https://doi.org/10.1016/j.jhazmat.2009.05.044.

20. Purnima, M.; Paul, T.; Pakshirajan, K.; Pugazhenthi, G. Onshore Oilfield Produced Water Treatment by Hybrid Microfiltration-Biological Process Using Kaolin Based Ceramic Membrane and Oleaginous Rhodococcus Opacus. *Chem. Eng. J.* **2023**, *453*, 139850. https://doi.org/10.1016/j.cej.2022.139850.

21. Chang, H.; Li, T.; Liu, B.; Vidic, R.D.; Elimelech, M.; Crittenden, J.C. Potential and Implemented Membrane-Based Technologies for the Treatment and Reuse of Flowback and Produced Water from Shale Gas and Oil Plays: A Review. *Desalination* **2019**, *455*, 34–57. https://doi.org/10.1016/j.desal.2019.01.001.

22. Yang, Y.; Tian, L.; Borch, T.; Tariq, H.; Li, T.; Bai, Y.; Su, Y.; Tiraferri, A.; Crittenden, J.C.; Liu, B. Safety and Technical Feasibility of Sustainable Reuse of Shale Gas Flowback and Produced Water after Advanced Treatment Aimed at Wheat Irrigation. *ACS Sustain. Chem. Eng.* **2022**, *10*, 12540–12551. https://doi.org/10.1021/acssuschemeng.2c02170.

23. Bagheri, M.; Roshandel, R.; Shayegan, J. Optimal Selection of an Integrated Produced Water Treatment System in the Upstream of Oil Industry. *Process Saf. Environ. Prot.* **2018**, *117*, 67–81. https://doi.org/10.1016/j.psep.2018.04.010.

24. Estrada, J.M.; Bhamidimarri, R. A Review of the Issues and Treatment Options for Wastewater from Shale Gas Extraction by Hydraulic Fracturing. *Fuel* **2016**, *182*, 292–303. https://doi.org/10.1016/j.fuel.2016.05.051.

25. Riley, S.M.; Oliveira, J.M.S.; Regnery, J.; Cath, T.Y. Hybrid Membrane Bio-Systems for Sustainable Treatment of Oil and Gas Produced Water and Fracturing Flowback Water. *Sep. Purif. Technol.* **2016**, *171*, 297–311. https://doi.org/10.1016/j.seppur.2016.07.008.

26. Ghafoori, S.; Omar, M.; Koutahzadeh, N.; Zendehboudi, S.; Malhas, R.N.; Mohamed, M.; Al-Zubaidi, S.; Redha, K.; Baraki, F.; Mehrvar, M. New Advancements, Challenges, and Future Needs on Treatment of Oilfield Produced Water: A State-of-the-Art Review. *Sep. Purif. Technol.* **2022**, *289*, 120652. https://doi.org/10.1016/j.seppur.2022.120652.

27. Alammar, A.; Park, S.-H.; Williams, C.J.; Derby, B.; Szekely, G. Oil-in-Water Separation with Graphene-Based Nanocomposite Membranes for Produced Water Treatment. *J. Membr. Sci.* **2020**, *603*, 118007. https://doi.org/10.1016/j.memsci.2020.118007.

28. Çakmakce, M.; Kayaalp, N.; Koyuncu, I. Desalination of Produced Water from Oil Production Fields by Membrane Processes. *Desalination* **2008**, *222*, 176–186. https://doi.org/10.1016/j.desal.2007.01.147.

29. Coday, B.D.; Xu, P.; Beaudry, E.G.; Herron, J.; Lampi, K.; Hancock, N.T.; Cath, T.Y. The Sweet Spot of Forward Osmosis: Treatment of Produced Water, Drilling Wastewater, and Other Complex and Difficult Liquid Streams. *Desalination* **2014**, *333*, 23–35. https://doi.org/10.1016/j.desal.2013.11.014.

30. Ebrahimi, M.; Willershausen, D.; Ashaghi, K.S.; Engel, L.; Placido, L.; Mund, P.; Bolduan, P.; Czermak, P. Investigations on the Use of Different Ceramic Membranes for Efficient Oil-Field Produced Water Treatment. *Desalination* **2010**, *250*, 991–996. https://doi.org/10.1016/j.desal.2009.09.088.

31. Maltos, R.A.; Regnery, J.; Almaraz, N.; Fox, S.; Schutter, M.; Cath, T.J.; Veres, M.; Coday, B.D.; Cath, T.Y. Produced Water Impact on Membrane Integrity During Extended Pilot Testing of Forward Osmosis–Reverse Osmosis Treatment. *Desalination* **2018**, *440*, 99–110. https://doi.org/10.1016/j.desal.2018.02.029.

32. Mat Nawi, N.I.; Bilad, M.R.; Anath, G.; Nordin, N.A.; Kurnia, J.C.; Wibisono, Y.; Arahman, N. The Water Flux Dynamic in a Hybrid Forward Osmosis-Membrane Distillation for Produced Water Treatment. *Membranes* **2020**, *10*, 225.

33. Munirasu, S.; Haija, M.A.; Banat, F. Use of Membrane Technology for Oil Field and Refinery Produced Water Treatment—A Review. *Process Saf. Environ. Prot.* **2016**, *100*, 183–202. https://doi.org/10.1016/j.psep.2016.01.010.

34. Padaki, M.; Surya Murali, R.; Abdullah, M.S.; Misdan, N.; Moslehyani, A.; Kassim, M.A.; Hilal, N.; Ismail, A.F. Membrane Technology Enhancement in Oil–Water Separation. A Review. *Desalination* **2015**, *357*, 197–207. https://doi.org/10.1016/j.desal.2014.11.023.

35. Ricceri, F.; Farinelli, G.; Giagnorio, M.; Zamboi, A.; Tiraferri, A. Optimization of Physico-Chemical and Membrane Filtration Processes to Remove High Molecular Weight Polymers from Produced Water in Enhanced Oil Recovery Operations. *J. Environ. Manag.* **2022**, *302*, 114015. https://doi.org/10.1016/j.jenvman.2021.114015.

36. Ricceri, F.; Giagnorio, M.; Farinelli, G.; Blandini, G.; Minella, M.; Vione, D.; Tiraferri, A. Desalination of Produced Water by Membrane Distillation: Effect of the Feed Components and of a Pre-Treatment by Fenton Oxidation. *Sci. Rep.* **2019**, *9*, 14964. https://doi.org/10.1038/s41598-019-51167-z.

37. Saqib Nawaz, M.; Alamoudi, T.; Soukane, S.; Soo Son, H.; Jin, Y.; Medina, S.C.; Mustakeem, M.; Gudideni, V.; Al-Qahtani, A.; Ghaffour, N. Performance and Implications of Forward Osmosis-Membrane Distillation Hybrid System for Simultaneous Treatment of Different Real Produced Water Streams. *Chem. Eng. J.* **2022**, *450*, 138479. https://doi.org/10.1016/j.cej.2022.138479.

38. Sardari, K.; Fyfe, P.; Ranil Wickramasinghe, S. Integrated Electrocoagulation–Forward Osmosis–Membrane Distillation for Sustainable Water Recovery from Hydraulic

Fracturing Produced Water. *J. Membr. Sci.* **2019**, *574*, 325–337. https://doi.org/10.1016/j.memsci.2018.12.075.

39. Thibault, Y.; Gamage McEvoy, J.; Mortazavi, S.; Smith, D.; Doiron, A. Characterization of Fouling Processes in Ceramic Membranes Used for the Recovery and Recycle of Oil Sands Produced Water. *J. Membr. Sci.* **2017**, *540*, 307–320. https://doi.org/10.1016/j.memsci.2017.06.065.

40. Zsirai, T.; Al-Jaml, A.K.; Qiblawey, H.; Al-Marri, M.; Ahmed, A.; Bach, S.; Watson, S.; Judd, S. Ceramic Membrane Filtration of Produced Water: Impact of Membrane Module. *Sep. Purif. Technol.* **2016**, *165*, 214–221. https://doi.org/10.1016/j.seppur.2016.04.001.

41. Chang, H.; Liu, B.; Wang, H.; Zhang, S.-Y.; Chen, S.; Tiraferri, A.; Tang, Y.-Q. Evaluating the Performance of Gravity-Driven Membrane Filtration as Desalination Pretreatment of Shale Gas Flowback and Produced Water. *J. Membr. Sci.* **2019**, *587*, 117187. https://doi.org/10.1016/j.memsci.2019.117187.

42. Chang, H.; Liu, S.; Tong, T.; He, Q.; Crittenden, J.C.; Vidic, R.D.; Liu, B. On-Site Treatment of Shale Gas Flowback and Produced Water in Sichuan Basin by Fertilizer Drawn Forward Osmosis for Irrigation. *Environ. Sci. Technol.* **2020**, *54*, 10926–10935. https://doi.org/10.1021/acs.est.0c03243.

43. Kusworo, T.D.; Aryanti, N.; Qudratun; Utomo, D.P. Oilfield Produced Water Treatment to Clean Water Using Integrated Activated Carbon-Bentonite Adsorbent and Double Stages Membrane Process. *Chem. Eng. J.* **2018**, *347*, 462–471. https://doi.org/10.1016/j.cej.2018.04.136.

44. Abdel-Shafy, H.I.; Mansour, M.S.M.; El-Toony, M.M. Integrated Treatment for Oil Free Petroleum Produced Water Using Novel Resin Composite Followed by Microfiltration. *Sep. Purif. Technol.* **2020**, *234*, 116058. https://doi.org/10.1016/j.seppur.2019.116058.

45. Lim, Y.J.; Lai, G.S.; Zhao, Y.; Ma, Y.; Torres, J.; Wang, R. A Scalable Method to Fabricate High-Performance Biomimetic Membranes for Seawater Desalination: Incorporating Pillar[5]Arene Wa ter Nanochannels into the Polyamide Selective Layer. *J. Membr. Sci.* **2022**, *661*, 120957. https://doi.org/10.1016/j.memsci.2022.120957.

46. Lim, Y.J.; Goh, K.; Kurihara, M.; Wang, R. Seawater Desalination by Reverse Osmosis: Current Development and Future Challenges in Membrane Fabrication—A Review. *J. Membr. Sci.* **2021**, *629*, 119292. https://doi.org/10.1016/j.memsci.2021.119292.

47. Ghaffour, N.; Soukane, S.; Lee, J.G.; Kim, Y.; Alpatova, A. Membrane Distillation Hybrids for Water Production and Energy Efficiency Enhancement: A Critical Review. *Appl. Energy* **2019**, *254*, 113698. https://doi.org/10.1016/j.apenergy.2019.113698.

48. Hizam, S.M.; Bilad, M.R.; Nordin, N.A.H.; Sambudi, N.S.; Wirzal, M.D.H.; Yusof, N.; Klaysom, C.; Jaafar, J. Inclined Forward Osmosis Module System for Fouling Control in Sustainable Produced Water Treatment Using Seawater as Draw Solution. *J. Water Process Eng.* **2021**, *40*, 101752. https://doi.org/10.1016/j.jwpe.2020.101752.

49. Li, L.; Shi, W.; Zang, L.; Wang, C.; Yu, S. Factors Affecting the Performance of Forward Osmosis Treatment for Oilfield Produced Water from Surfactant-Polymer Flooding. *J. Membr. Sci.* **2020**, *615*, 118457. https://doi.org/10.1016/j.memsci.2020.118457.

50. Liden, T.; Carlton, D.D.; Miyazaki, S.; Otoyo, T.; Schug, K.A. Forward Osmosis Remediation of High Salinity Permian Basin Produced Water from Unconventional Oil and Gas Development. *Sci. Total Environ.* **2019**, *653*, 82–90. https://doi.org/10.1016/j.scitotenv.2018.10.325.

51. Liden, T.; Carlton, D.D.; Miyazaki, S.; Otoyo, T.; Schug, K.A. Comparison of the Degree of Fouling at Various Flux Rates and Modes of Operation Using Forward Osmosis for Remediation of Produced Water from Unconventional Oil and Gas Development. *Sci. Total Environ.* **2019**, *675*, 73–80. https://doi.org/10.1016/j.scitotenv.2019.04.061.

52. Minier-Matar, J.; Hussain, A.; Janson, A.; Wang, R.; Fane, A.G.; Adham, S. Application of Forward Osmosis for Reducing Volume of Produced/Process Water from Oil and Gas Operations. *Desalination* **2015**, *376*, 1–8. https://doi.org/10.1016/j.desal.2015.08.008.

53. Nawaz, M.S.; Son, H.S.; Jin, Y.; Kim, Y.; Soukane, S.; Al-Hajji, M.A.; Abu-Ghdaib, M.; Ghaffour, N. Investigation of Flux Stability and Fouling Mechanism During Simultaneous Treatment of Different Produced Water Streams Using Forward Osmosis and Membrane Distillation. *Water Res.* **2021**, *198*, 117157. https://doi.org/10.1016/j.watres.2021.117157.

54. Silva, T.L.S.; Morales-Torres, S.; Castro-Silva, S.; Figueiredo, J.L.; Silva, A.M.T. An Overview on Exploration and Environmental Impact of Unconventional Gas Sources and Treatment Options for Produced Water. *J. Environ. Manag.* **2017**, *200*, 511–529. https://doi.org/10.1016/j.jenvman.2017.06.002.

55. Abousnina, R.M.; Nghiem, L.D. Removal of Dissolved Organics from Produced Water by Forward Osmosis. *Desalin. Water Treat.* **2014**, *52*, 570–579. https://doi.org/10.1080/19443994.2013.827292.

56. Ahmadizadeh, R.; Shokrollahzadeh, S.; Latifi, S.M. Forward Osmosis Performance in Extracting Water from Produced Water. *J. Appl. Water Eng. Res.* **2022**, *10*, 78–86. https://doi.org/10.1080/23249676.2021.1958712.

57. Al Hawli, B.; Benamor, A.; Hawari, A.A. A Hybrid Electro-Coagulation/Forward Osmosis System for Treatment of Produced Water. *Chem. Eng. Process. Process Intensif.* **2019**, *143*, 107621. https://doi.org/10.1016/j.cep.2019.107621.

58. Bell, E.A.; Poynor, T.E.; Newhart, K.B.; Regnery, J.; Coday, B.D.; Cath, T.Y. Produced Water Treatment Using Forward Osmosis Membranes: Evaluation of Extended-Time Performance and Fouling. *J. Membr. Sci.* **2017**, *525*, 77–88. https://doi.org/10.1016/j.memsci.2016.10.032.

59. Coday, B.D.; Almaraz, N.; Cath, T.Y. Forward Osmosis Desalination of Oil and Gas Wastewater: Impacts of Membrane Selection and Operating Conditions on Process Performance. *J. Membr. Sci.* **2015**, *488*, 40–55. https://doi.org/10.1016/j.memsci.2015.03.059.

60. Coday, B.D.; Cath, T.Y. Forward Osmosis: Novel Desalination of Produced Water and Fracturing Flowback. *J. AWWA* **2014**, *106*, E55–E66. https://doi.org/10.5942/jawwa.2014.106.0016.

61. Giagnorio, M.; Ricceri, F.; Tiraferri, A. Desalination of Brackish Groundwater and Reuse of Wastewater by Forward Osmosis Coupled with Nanofiltration for Draw Solution Recovery. *Water Res.* **2019**, *153*, 134–143. https://doi.org/10.1016/j.watres.2019.01.014.

62. Ang, W.L.; Mohammad, A.W.; Hilal, N.; Leo, C.P. A Review on the Applicability of Integrated/Hybrid Membrane Processes in Water Treatment and Desalination Plants. *Desalination* **2015**, *363*, 2–18. https://doi.org/10.1016/j.desal.2014.03.008.

63. Camilleri-Rumbau, M.S.; Nguyen, X.T.; Sanahuja-Embuena, V.; Frauholz, J.; Yangali Quintanilla, V.A.; Tiraferri, A.; Petrinic, I.; Helix-Nielsen, C. Forward Osmosis. In *Experimental Methods for Membrane Applications in Desalination and Water Treatment*; Salinas-Rodríguez, S.G., Villacorte, L.O., Eds.; IWA Publishing: London, UK, 2024.

64. Bhinder, A.; Fleck, B.A.; Pernitsky, D.; Sadrzadeh, M. Forward Osmosis for Treatment of Oil Sands Produced Water: Systematic Study of Influential Parameters. *Desalin. Water Treat.* **2016**, *57*, 22980–22993. https://doi.org/10.1080/19443994.2015.1108427.

65. Chen, G.; Wang, Z.; Nghiem, L.D.; Li, X.-M.; Xie, M.; Zhao, B.; Zhang, M.; Song, J.; He, T. Treatment of Shale Gas Drilling Flowback Fluids (Sgdfs) by Forward Osmosis: Membrane Fouling and Mitigation. *Desalination* **2015**, *366*, 113–120. https://doi.org/10.1016/j.desal.2015.02.025.

66. Tiraferri, A.; Yip, N.Y.; Straub, A.P.; Romero-Vargas Castrillon, S.; Elimelech, M. A Method for the Simultaneous Determination of Transport and Structural Parameters of Forward Osmosis Membranes. *J. Membr. Sci.* **2013**, *444*, 523–538. https://doi.org/10.1016/j.memsci.2013.05.023.

67. Giagnorio, M.; Ricceri, F.; Tagliabue, M.; Zaninetta, L.; Tiraferri, A. Hybrid Forward Osmosis–Nanofiltration for Wastewater Reuse: System Design. *Membranes* **2019**, *9*, 61.

68. Giagnorio, M.; Morciano, M.; Zhang, W.; Hélix-Nielsen, C.; Fasano, M.; Tiraferri, A. Coupling of Forward Osmosis with Desalination Technologies: System-Scale Analysis at the Water-Energy Nexus. *Desalination* **2022**, *543*, 116083. https://doi.org/10.1016/j.desal.2022.116083.

69. Giagnorio, M.; Casasso, A.; Tiraferri, A. Environmental Sustainability of Forward Osmosis: The Role of Draw Solute and Its Management. *Environ. Int.* **2021**, *152*, 106498. https://doi.org/10.1016/j.envint.2021.106498.

70. Kegl, T.; Korenak, J.; Bukšek, H.; Petrinić, I. Modeling and Multi-Objective Optimization of Forward Osmosis Process. *Desalination* **2024**, *580*, 117550. https://doi.org/10.1016/j.desal.2024.117550.

71. Altaee, A.; Hilal, N. High Recovery Rate Nf–Fo–Ro Hybrid System for Inland Brackish Water Treatment. *Desalination* **2015**, *363*, 19–25. https://doi.org/10.1016/j.desal.2014.12.017.

72. Kim, J.; Kim, J.; Kim, J.; Hong, S. Osmotically Enhanced Dewatering-Reverse Osmosis (Oed-Ro) Hybrid System: Implications for Shale Gas Produced Water Treatment. *J. Membr. Sci.* **2018**, *554*, 282–290. https://doi.org/10.1016/j.memsci.2018.03.015.

73. Blandin, G.; Verliefde, A.R.D.; Tang, C.Y.; Le-Clech, P. Opportunities to Reach Economic Sustainability in Forward Osmosis–Reverse Osmosis Hybrids for Seawater Desalination. *Desalination* **2015**, *363*, 26–36. https://doi.org/10.1016/j.desal.2014.12.011.

74. Wagner, R., & Judd, B. (2006). Fundamentals-gas sweetening. In *PROCEEDINGS OF THE LAURANCE REID GAS CONDITIONING CONFERENCE* (Vol. 2006, p. 1).

75. Liu, Y., Liu, Z., Morisato, A., Bhuwania, N., Chinn, D., & Koros, W. J. (2020). Natural gas sweetening using a cellulose triacetate hollow fiber membrane illustrating controlled plasticization benefits. *Journal of membrane science*, *601*, 117910.

76. Salim, S. R. S. (2021, March). Treatment of amine wastes generated in industrial processes. In *IOP Conference Series: Materials Science and Engineering* (Vol. 1092, No. 1, p. 012051). IOP Publishing.

77. Halim, M., Kadirkhan, F., Mustapa, W. N. F. W., Soh, W. K., & Yeo, S. (2020). Natural gas sweetening polymeric membrane: Established optimum operating condition at 70% of CO2 concentration feed gas stream. *Malays. J. Fundam. Appl. Sci*, *16*, 54-58.

78. Pasichnyk, M., Stanovsky, P., Polezhaev, P., Zach, B., Šyc, M., Bobák, M., ... & Izák, P. (2023). Membrane technology for challenging separations: Removal of CO2, SO2 and NOX from flue and waste gases. *Separation and Purification Technology*, 124436.

79. Ghasem, N., & Nihmiya, A. R. (2024). Modeling and simulation of natural gas sweetening using membranes. In *Advances Natural Gas: Formation, Processing, and Applications. Volume 8: Natural Gas Process Modelling and Simulation* (pp. 81-103). Elsevier.

80. Islam, M. S., Yusoff, R., Ali, B. S., Islam, M. N., & Chakrabarti, M. H. (2011). Degradation studies of amines and alkanolamines during sour gas treatment process. *International Journal of Physical Sciences*, *6*(25), 5883-5896.

81. Zabiri, H., & Kamaruddin, B. (2024). Case studies of modeling and simulation of natural gas sweetening processes. *Advances Natural Gas: Formation, Processing, and Applications. Volume 8: Natural Gas Process Modelling and Simulation*, 145-161.

82. Ahmad, A. L., Zainuddin, M. I. F., & Buddin, M. M. H. S. (2024). Polymeric membranes for natural gas sweetening. In *Advances in Natural Gas: Formation, Processing, and Applications. Volume 2: Natural Gas Sweetening* (pp. 419-452). Elsevier.

83. Simmons, C. V. (1991). Reclaiming used amine and glycol solutions. In *Proceedings of Laurance Reid Gas Conditioning Conference Norman*.

84. Ellaf, A., Taqvi, S. A. A., Zaeem, D., Siddiqui, F. U. H., Kazmi, B., Idris, A., ... & Mushab, M. S. S. (2023). Energy, exergy, economic, environment, exergo-environment based assessment of amine-based hybrid solvents for natural gas sweetening. *Chemosphere*, *313*, 137426.

85. Tikadar, D., Gujarathi, A. M., & Guria, C. (2023). Towards retrofitting based multi-criteria analysis of an industrial gas sweetening process: Further insights of CO2 emissions. *Process Safety and Environmental Protection*, *175*, 259-271.

86. Gonfa, G., & Ullah, S. (2024). Natural gas sweetening by ionic liquid membranes. In *Advances in Natural Gas: Formation, Processing, and Applications. Volume 2: Natural Gas Sweetening* (pp. 453-470). Elsevier.

87. Serio, M. A., Kroo, E., Bassilakis, R., Wójtowicz, M. A., & Suuberg, E. M. (2001). *A prototype pyrolyzer for solid waste resource recovery in space* (No. 2001-01-2349). SAE Technical Paper.

88. Mohajeri, M., Panahi, M., & Shahsavand, A. (2024). Optimal operation of a natural gas sweetening plant. *Computers & Chemical Engineering*, 108631.

89. Taqvi, S. A. A., & Ellaf, A. (2024). Introduction to natural gas sweetening methods and technologies. In *Advances in Natural Gas: Formation, Processing, and Applications. Volume 2: Natural Gas Sweetening* (pp. 3-32). Elsevier.

90. Ahmed, S. F., Mehejabin, F., Momtahin, A., Tasannum, N., Faria, N. T., Mofijur, M., ... & Mahlia, T. M. I. (2022). Strategies to improve membrane performance in wastewater treatment. *Chemosphere*, *306*, 135527.

91. Yusuf, A., Sodiq, A., Giwa, A., Eke, J., Pikuda, O., De Luca, G., ... & Chakraborty, S. (2020). A review of emerging trends in membrane science and technology for sustainable water treatment. *Journal of cleaner production*, *266*, 121867.

92. Lutchmiah, K., Verliefde, A. R. D., Roest, K., Rietveld, L. C., & Cornelissen, E. R. (2014). Forward osmosis for application in wastewater treatment: A review. *Water research*, *58*, 179-197.

93. Wang, J., & Liu, X. (2021). Forward osmosis technology for water treatment: Recent advances and future perspectives. *Journal of Cleaner Production*, *280*, 124354.

94. Ibrar, I., Altaee, A., Zhou, J. L., Naji, O., & Khanafer, D. (2020). Challenges and potentials of forward osmosis process in the treatment of wastewater. *Critical reviews in environmental science and technology*, *50*(13), 1339-1383.

95. Cath, T. Y., Childress, A. E., & Elimelech, M. (2006). Forward osmosis: Principles, applications, and recent developments. *Journal of membrane science*, *281*(1-2), 70-87.

96. Botheju, D., Glarborg, P., & Tokheim, L. A. (2013). The use of amine reclaimer wastes as a NOx reduction agent. *Energy Procedia*, *37*, 691-700.

97. PETRUS, F. (1997). Process for the purification of an alkanolamine (Patent No. 1998137786). Shell Internationale Research Maatschappij. https://patentscope.wipo.int/search/en/detail.jsf?docId=EP13169334&_cid=P11-LVVMLH-59411-1

98. Madaeni, S. S. (1999). The application of membrane technology for water disinfection. *Water Research*, *33*(2), 301-308.

99. Ungerer, B. (2012). Method of treatment of amine wastewater and a system for accomplishing the same (U.S. Patent No. 20130220792). https://patentscope.wipo.int/search/en/detail.jsf?docId=US90515118&_cid=P11-LVVN0A-67075-1

100. Edward, C. (1992). Method of forming strip products from thermoplastic materials (U.S. Patent No. 5171499). https://patentscope.wipo.int/search/en/detail.jsf?docId=US38160692&_cid=P11-LVVN7E-70812-1

101. Jean, N. (1990). Composition membrane for separating water from fluids containing organic components by means of pervaporation (U.S. Patent No. 5334314). https://patentscope.wipo.int/search/en/detail.jsf?docId=US38382178&_cid=P11-LVVNB7-72831-1

102. Luise, S. (1990). removal of water from a mixture of water, CO.sub.2 and amines (U.S. Patent No. 5051188). https://patentscope.wipo.int/search/en/detail.jsf?docId=US38004953&_cid=P11-LVVNEX-74710-1

103. KOICHI, S. (1998). Amines-Containing Waste Liquid Treatment And Device Therefor (Japan Patent No. 1998137786). https://patentscope.wipo.int/search/en/detail.jsf?docId=JP267584608&_cid=P21-L4X6GO-43554-1

104. NORIHIKO, Y. (2008). Method Of Treating Aromatic Amines-Containing Wastewater (Japan Patent No. 2010131489). https://patentscope.wipo.int/search/en/detail.jsf?docId=JP272111221&_cid=P21-L4X6KN-44486-1

105. BOONG IK, J. (2013). Nitrogen Wastewater Treatment Facility Capable Of Converting Amines In Wastewater To Ammonia Through A Biological Treatment And Separating The Ammonia Through Aeration, And A Method Thereof (Republic of Korea Patent No. 1020130095038). https://patentscope.wipo.int/search/en/detail.jsf?docId=KR95474269&_cid=P21-L4X6MC-44927-1

106. BHUWANIA, N. (2019). Forming Diluted Brine Without Addition Of Soft Or Contaminated Water In An Oil And Gas Treatment Facility (U.S. Patent No. 20190263685). https://patentscope.wipo.int/search/en/detail.jsf?docId=US251053056&_cid=P20-L88PA7-26169-2

107. HUI, D. (2017). Preparation method for forward osmosis membrane and method for treating pesticide wastewater by using forward osmosis membrane (China Patent No. 107413196). https://patentscope.wipo.int/search/en/detail.jsf?docId=CN207737125&_cid=P20-L88N04-96074-1

108. HERRON, John R. (2012). Food Waste Concentration System And Related Processes (U.S. Patent No. 2012106732). https://patentscope.wipo.int/search/en/detail.jsf?docId=WO2012106732&_cid=P20-L88PA7-26169-1

109. RAHAMAN, S. (2020). Membranes For Forward Osmosis And Membrane Distillation And Process Of Treating Fracking Wastewater (Canada Patent No. 2020056508). https://patentscope.wipo.int/search/en/detail.jsf?docId=WO2020056508&_cid=P20-L88PA7-26169-2

110. Hua Ho, C. (2022). SYSTEM AND METHOD OF TREATING WASTE WATER (U.S. Patent No. 20220204375).https://patentscope.wipo.int/search/en/detail.jsf?docId=US366839623&_cid=P20-L88PA7-26169-3

111. Oh, G. T., Ahn, C. K., & Lee, M. W. (2022). Advanced oxidation pretreatment for biological treatment of reclaimer wastewater containing high concentration N-methyldiethanolamine. *Applied Sciences*, *12*(8), 3960.

112. Fürhacker, M., Pressl, A., & Allabashi, R. (2003). Aerobic biodegradability of methyldiethanolamine (MDEA) used in natural gas sweetening plants in batch tests and continuous flow experiments. *Chemosphere*, *52*(10), 1743-1748.

113. Campo, P., Platten III, W., Suidan, M. T., Chai, Y., & Davis, J. W. (2011). Aerobic biodegradation of amines in industrial saline wastewaters. *Chemosphere*, *85*(7), 1199-1203.

114. Libralato, G., Ghirardini, A. V., & Avezzu, F. (2008). Evaporation and air-stripping to assess and reduce ethanolamines toxicity in oily wastewater. *Journal of hazardous materials*, *153*(3), 928-936.

115. Zoannou, K. S., Sapsford, D. J., & Griffiths, A. J. (2013). Thermal degradation of monoethanolamine and its effect on CO2 capture capacity. *International Journal of Greenhouse Gas Control*, *17*, 423-430.

116. Pinheiro, C. T., Ascensão, V. R., Cardoso, C. M., Quina, M. J., & Gando-Ferreira, L. M. (2017). An overview of waste lubricant oil management system: Physicochemical characterization contribution for its improvement. *Journal of Cleaner Production*, *150*, 301-308.

117. Pinheiro, C. T., Quina, M. J., & Gando-Ferreira, L. M. (2021). Management of waste lubricant oil in Europe: A circular economy approach. *Critical Reviews in Environmental Science and Technology*, *51*(18), 2015-2050.

118. Diphare, M. J., Pilusa, J., Muzenda, E., & Mollagee, M. (2013, August 25-26). A Review of Waste Lubricating Grease Management. 2nd International Conference on Environment, Agriculture and Food Sciences (ICEAFS'2013), Kuala Lumpur, Malaysia. https://api.semanticscholar.org/CorpusID:38915437

119. Parekh, K., Gaur, R., & Shahabuddin, S. (2024). A facile approach for refining waste lubricant oil: A hazardous water contaminant. *Materials Today: Proceedings*.

120. Zhu, H., Chen, K., Sun, G., Zhao, W., Jiang, Q., & Xiao, C. (2023). Robust design of durable PTFE/graphene hollow fiber composite membrane for high-temperature lubricant recycling. *Journal of Water Process Engineering*, *55*, 104163.

121. Cao, D., Gai, L., Niu, D., Li, Y., Li, J., Tian, R., & Li, K. (2022). Purification of Camellia Oil by Inorganic Ceramic Membrane. *Foods*, *11*(22), 3644.

122. Moses, K. K., Aliyu, A., Hamza, A., & Mohammed-Dabo, I. A. (2023). Recycling of waste lubricating oil: A review of the recycling technologies with a focus on catalytic cracking, techno-economic and life cycle assessments. *Journal of Environmental Chemical Engineering*, *11*(6), 111273.

123. Guerin, T. F. (2008). Environmental liability and life-cycle management of used lubricating oils. *Journal of Hazardous Materials*, *160*(2-3), 256-264.

124. Yang, Y., Wang, C., Xue, Y., Yan, J., & Han, S. (2022). Decolorization and Regeneration of Waste Lubricating Oil by a CNTs/PDMS/PVDF Membrane. *Energy Sources, Part A: Recovery, Utilization, and Environmental Effects*, 1–10. https://doi.org/10.1080/15567036.2022.2041132

125. Jafari, A. J., & Hassanpour, M. (2015). Analysis and comparison of used lubricants, regenerative technologies in the world. *Resources, Conservation and Recycling*, *103*, 179-191.

126. Willing, A. (2001). Lubricants based on renewable resources–an environmentally compatible alternative to mineral oil products. *Chemosphere*, *43*(1), 89-98.

127. Pramanik, K. (2003). Properties and use of Jatropha curcas oil and diesel fuel blends in compression ignition engine. *Renewable energy*, *28*(2), 239-248.

128. Hu, G., Li, J., & Zeng, G. (2013). Recent development in the treatment of oily sludge from petroleum industry: a review. *Journal of hazardous materials*, *261*, 470-490.

129. Mynin, V. N., Smirnova, E. B., Katsereva, O. V., Komyagin, E. A., Terpugov, G. V., & Smirnov, V. N. (2004). Treatment and regeneration of used lube oils with inorganic membranes. *Chemistry and Technology of Fuels and Oils*, *40*, 345-350.

130. Widodo, S., Ariono, D., Khoiruddin, K., Hakim, A. N., & Wenten, I. G. (2018). Recent advances in waste lube oils processing technologies. *Environmental Progress & Sustainable Energy*, *37*(6), 1867-1881.

131. Audibert, F. (2006). Oil Composition and required treatment steps. *Waste Engine Oils: Rerefining and Energy Recovery* (pp.35-86). Netherlands: Elsevier B.V.

132. El-Mekkawi, S. A., El-Ibiari, N. N., Attia, N. K., El-Diwani, G. I., El-Ardy, O. A., & El Morsi, A. K. (2020). Reducing the environmental impact of used lubricating oil through the production of fuels by pyrolysis. *Environmental nanotechnology, monitoring & management*, *14*, 100308.

133. Sri, R. (2011, July 22-23). Lubricating Oil Waste Purification with Ultrafiltration Membrane. Bali International Seminar on Science And Technology, Bali, Indonesia. https://core.ac.uk/download/pdf/19892273.pdf

134. Gourgouillon, D., Schrive, L., Sarrade, S., & Rios, G. M. (2000). An environmentally friendly process for the regeneration of used oils. *Environmental Science & Technology*, *34*(16), 3469-3473.

135. Ciora, R. J., & Liu, P. K. (2003). Ceramic membranes for environmental related applications. *Fluid/Particle Separation Journal*, *15*(1), 51-60.

136. Psoch, C., Wendler, B., Goers, B., Wozny, G., & Ruschel, B. (2004). Waste oil conditioning via microfiltration with ceramic membranes in cross flow. *Journal of Membrane Science*, *245*(1-2), 113-121.

137. Wenten, I. G. (2005). Recent development in membrane and its industrial applications. *Membrane Technology in Oil and Gas Industry*.

138. Yu, M., Ma, H., & Wang, Q. (2012). Research and recycling advancement of used oil in China and all over the World. *Procedia Environmental Sciences*, *16*, 239-243.

139. White, L. S., & Nitsch, A. R. (2000). Solvent recovery from lube oil filtrates with a polyimide membrane. *Journal of Membrane Science*, *179*(1-2), 267-274.

140. European Commission (n.d.). *Customised membranes for green and resilient industries*. CUMERI. 2023, April 10. https://cumeri.eu/

141. Widodo, S., Khoiruddin, K., Ariono, D., Subagjo, S., & Wenten, I. G. (2020). Re-refining of waste engine oil using ultrafiltration membrane. *Journal of Environmental Chemical Engineering*, *8*(3), 103789.

142. Nissar, A., Hanief, M., Mir, F. Q., Nissar, A., Hanief, M., & Mir, F. Q. (2024). Recycling of waste lubricating oil using ultra filtration membrane and modeling and prediction of its rheological behavior using Gauss-Newton algorithm.

143. Cao, Y., Yan, F., Li, J., Liang, X., & He, B. (2009). Used lubricating oil recycling using a membrane filtration: analysis of efficiency, structural and composing, Desalin. Water Treat. 2009; 11: 1-3 73-80.

144. Mustafa, G., Wyns, K., Buekenhoudt, A., & Meynen, V. (2016). New insights into the fouling mechanism of dissolved organic matter applying nanofiltration membranes with a variety of surface chemistries. *Water research*, *93*, 195-204.

145. Mustafa, G., Wyns, K., Vandezande, P., Buekenhoudt, A., & Meynen, V. (2014). Novel grafting method efficiently decreases irreversible fouling of ceramic nanofiltration membranes. *Journal of Membrane Science*, *470*, 369-377.

146. Kim, J. B., Huang, W., Miller, M. D., Baker, G. L., & Bruening, M. L. (2003). Kinetics of surface-initiated atom transfer radical polymerization. *Journal of Polymer Science Part A: Polymer Chemistry*, *41*(3), 386-394.

147. Hosseinabadi, S. R., Wyns, K., Meynen, V., Carleer, R., Adriaensens, P., Buekenhoudt, A., & Van der Bruggen, B. (2014). Organic solvent nanofiltration with Grignard functionalised ceramic nanofiltration membranes. *Journal of Membrane Science*, *454*, 496-504.

148. Mohammadi, T., & Safavi, M. A. (2009). Application of Taguchi method in optimization of desalination by vacuum membrane distillation. *Desalination*, *249*(1), 83-89.

149. Marenchino, R., Pagliero, C., & Mattea, M. (2006). Vegetable oil degumming using inorganic membranes. *Desalination*, *200*(1-3), 562-564.